RSC Sustainability

ROYAL SOCIETY OF CHEMISTRY

PAPER

View Article Online
View Journal | View Issue

Cite this: *RSC Sustainability*, 2025, **3**, 4632

Sustainability analysis of electrochemical direct air capture technologies

Grazia Leonzio *[ab] and Nilay Shah[b]

Global warming caused by anthropogenic greenhouse gas emissions, particularly carbon dioxide in the atmosphere, has garnered significant attention due to its detrimental environmental impacts. Carbon capture from both point and dilute sources is amongst the critical technologies needed to mitigate these negative phenomena. Carbon dioxide capture from flue gas is a well-established technology, while carbon capture from the air through direct air capture processes remains under research and development. In recent years, attention has focused on fully electrified direct air capture systems as potential candidates for large-scale direct air capture applications capable of exploiting renewable energy sources. However, economic and environmental analyses are missing in the literature. In this work, a scale-up analysis of different electrified direct air capture technologies (based on electrolysis, bipolar membrane electrodialysis, electro-swing adsorption, and proton-coupled electron transfer systems) is conducted through a hybrid learning curve methodology in order to evaluate total costs and environmental impact (according to scopes 1 and 2). The analysis is conducted for different geographic locations, times of year, and types of renewable energy source. Results show that electro-swing adsorption and proton-coupled electron transfer processes are both characterized by lower costs and environmental burdens, while electrolysis and electrodialysis systems have higher costs and environmental impacts. A technique for order preference by similarity to ideal solution analysis is carried out to determine the most sustainable process considering technical, economic, social, and environmental aspects. Results indicate that the proton coupled electron transfer system, built in China, in 2040–2050, exploiting wind offshore energy is the most sustainable process.

Received 30th March 2025
Accepted 4th August 2025

DOI: 10.1039/d5su00227c

rsc.li/rscsus

Sustainability spotlight

Direct Air Capture (DAC) is an emerging form of atmospheric carbon dioxide removal. Conventional DAC utilizes thermal energy for the regeneration step, which is energy-intensive and hinders large-scale deployment. For these reasons, electrically driven DAC technologies have been investigated and proposed in the literature, but a deep techno-economic and environmental analysis on a large scale is missing. In this work, a scale-up of these fully electrified DAC systems is carried out for different regions around the world, different years and renewable energy sources.

1 Introduction

It is an obvious fact that carbon dioxide (CO_2) emissions that have accumulated in the atmosphere as a result of human activities cause significant damage to the environment, leading to the increase of temperatures and climate change, causing the shrinking of ice sheets, rising sea level, and more extreme natural events.[1] As the most prevalent greenhouse gas (GHG), it was determined that global CO_2 emissions were 37.79 billion tons in 2023,[2] achieving an atmospheric concentration of 419.3 ppm.[3] The increase between 2022 and 2023 was 2.8 ppm (the 12th year in a row where the amount of CO_2 in the atmosphere increased by more than 2 ppm). Around the world, China, Europe, and the United States are the regions with the highest CO_2 emissions of 11.9 billion tons, 2.51 billion tons, and 4.91 billion tons, respectively, measured in 2023.[2]

Climate experts have warned that "If emissions of all greenhouse gases to the atmosphere were to stop today, though very unlikely, the climate impacts of the existing concentrations of N_2O and CH_4 in the atmosphere would dissipate in a few decades, whereas the existing CO_2 in the atmosphere would remain behind to warm the globe for centuries to come"; thus, urgent actions are required.[4]

According to the Intergovernmental Panel on Climate Change (IPCC), it is important to decrease CO_2 emissions and particularly aim for net-zero emissions by 2050 through decarbonization, curbing fossil fuel consumption and CO_2 emissions, and removing CO_2.[5] The last cited solution, *e.g.*, the

[a]*Department of Mechanical, Chemical and Materials Engineering, Cagliari University, Via Marengo 2, 09123 Cagliari, Italy. E-mail: grazia.leonzio@unica.it*
[b]*Department of Chemical Engineering, Sargent Centre for Process Systems Engineering, Imperial College London, SW7 2AZ London, UK*

removal of CO_2, is carried out through the so-called carbon dioxide removal (CDR) techniques: afforestation and reforestation, biochar, soil carbon sequestration, enhanced weathering, ocean alkalinization, biomass with carbon removal and storage (BiCRS), and direct air capture (DAC).[6] All of them aim explicitly to reduce CO_2 levels and are emerging as a crucial process that helps to achieve carbon neutrality and negative CO_2 emissions.[7,8] However, currently, almost all CDR technologies still require dedicated efforts to make them economically appealing and less energy-demanding.[9] Among the CDR technologies, DAC, capturing CO_2 directly from the atmosphere where its concentration is much lower compared to point sources, is attracting more and more interest since it fits the target of net negative emissions and has the advantage of high flexibility in operation location and time.[10,11] DAC technologies include absorption, adsorption, mineral carbonation, membranes, photocatalysis, and cryogenic separation.[12] Absorption and adsorption technologies are the most analyzed, established, and studied in the literature.[13–15] All these cited technologies are based on using thermal energy and cycles and are currently high-cost technologies with 5–10 GJ required to capture a ton of atmospheric CO_2.[16] However, it would be highly desirable to regenerate DAC materials with low-cost, zero-carbon energy.

For this reason, in recent years, DAC technologies based on renewable and electrical energy consumption have been investigated in the literature, including bipolar membrane electrodialysis (BPMED), electrolysis, electro-swing adsorption (ESA), proton-coupled electron transfer (PCET), electrochemically-mediated amine regeneration (EMAR)-based technology, and systems using redox-active organic materials (quinones, bipyridines, thiolates, *etc.*) or transition metals.[16–18] Electrolysis, BPMED, and PCET systems are based on pH-swing operating principles since CO_2 solubility is dependent on the pH value (CO_2 is captured and released at high and low pH values, respectively), so that pH changes convert (bi)carbonates into dissolved CO_2. In most cases, BPMED and electrochemical cells are linked to an absorption column capturing CO_2 from the air and are used for both solvent regeneration and CO_2 release.[19,20]

The advantages of a fully electrified DAC (e-DAC) technology are as follows: not relying on energy-intensive heat and pressure; it can work with 100% of renewable power sources and potentially requires a smaller physical footprint than the complex mechanical processes used in conventional DAC; it can operate at ambient temperature and pressure; it is characterized by scalability and modularity.[21] CO_2 capture systems based on electrochemistry may play a key role in the development of next-generation technologies, and new companies are emerging in this field (Mission Zero, Carbon Atlantis, E-quester, Repair, Verdox, and RedoxNRG).[21–27]

E-DAC processes have been recently investigated in the literature, mostly from an experimental point of view to measure efficiency and feasibility, even though a few mathematical models have been developed.

Regarding the e-DAC technology based on electro-swing adsorption, Hemmatifar *et al.*[28] developed and constructed a modular, expandable, and easy-to-fabricate cell stack with poly(vinylanthraquinone)-carbon nanotube (PVAQ-CNT) composite cathodes and poly(vinylferrocene)-CNT (PVFc-CNT) composite anodes. Reduction and oxidation of quinone at the cathode site allow the capture and release of CO_2, respectively. In particular, results show its feasibility for CO_2 capture at a low concentration (400 ppm) with an energy consumption as low as 113 kJ per mol CO_2 after 7 cycles. This study was based on that of Voskian and Hatton,[29] where the ESA system, composed of a polyanthraquinone-CNT (PAQCNT) composite as the cathode, polyvinylferrocene-CNT (PVFc-CNT) composite as the anode in [Bmim][TF2N] ionic liquid, showed in experimental analysis a stability after 7000 cycles with 90% faradaic efficiency, 100% bed utilization, and an energy consumption of 90 kJ $mol_{CO_2}^{-1}$.

The PCET technology was also investigated in the literature. Xie *et al.*[30] found experimentally that the use of an optimal derivative (7,8-dihydroxyphenazine-2-sulfonic acid) with high solubility, fast kinetics, and stability ensures 95.8% current efficiency at 10 mA cm^{-2} and a low energy consumption of 0.49 GJ $ton_{CO_2}^{-1}$. A similar analysis was conducted by Jin *et al.*[31] using 3,3′-(phenazine-2,3-diylbis(oxy))bis(propane-1-sulfonate) molecules in an experimental PCET system (a flow cell with electrochemically induced pH swings). The authors established an energy consumption ranging between 121 and 237 kJ per mol_{CO_2} at 20 mA cm^{-2}. The same authors presented a new hybrid flow cell, where redox-active phenazine molecules are integrated into solid electrode materials instead of being dissolved in a solution, requiring an energy duty of 126 kJ $mol_{CO_2}^{-1}$ for atmospheric air and 73 kJ $mol_{CO_2}^{-1}$ for simulated flue gas.[32] The system has the advantage of operating with a high coulombic efficiency (about 99%), meaning a high stability to oxygen. Research on the evaluation of the minimum work and comparison among redox compounds has also been conducted. In particular, the ideal cycle work for a PCET system using sodium 3,30-(phenazine-2,3-diylbis(oxy))bis(propane-1-sulfonate) as the proton carrier in an aqueous solution was evaluated by Jin *et al.*[33] through a thermodynamic analysis, finding a range between 20 and 70 kJ $mol_{CO_2}^{-1}$. A comparison among organic (1-aminopyridinium and neutral red) and inorganic (manganese oxide) redox active compounds for pH swing was proposed by Seo *et al.*[34] Results show that although inorganic materials have a higher stability compared to organic ones, they are characterized by a limited surface area-to-volume ratio, requiring a careful electrode design. A more accurate analysis was experimentally conducted by Seo and Hatton,[35] considering neutral red as a redox active material (because it is oxygen insensitive) and determining that for a continuous flow cell fed by ambient air (410 ppm in CO_2 concentration), electron utilization and energy consumption were respectively 38% and 65 kJ $mol_{CO_2}^{-1}$.

Regarding electrolytic cells, Shu *et al.*[36] built an experimental setup for an electrolytic cell that was used to simultaneously regenerate the NaOH aqueous solution and release the captured CO_2. Results show that the energy consumption, CO_2 purity, and minimum energy consumption were, respectively, 374 kJ $mol_{CO_2}^{-1}$, higher than 95% and 164 kJ $mol_{CO_2}^{-1}$. An energy requirement of the same order of magnitude (*e.g.*, 240 kJ $mol_{CO_2}^{-1}$) was obtained by Muroyama and Gubler[37] who developed and demonstrated an anion exchange membrane cell

releasing CO_2 from the carbonates of an absorption column. Shu *et al.*[38] investigated solutions to reduce energy consumption by considering a partial vacuum in the gas phase during CO_2 desorption or adding a background electrolyte (phosphate or sulphate) to the alkaline absorbent. The results show that the lowest energy consumption of 247 kJ $mol_{CO_2}^{-1}$ can be achieved with 0.3 atm as the CO_2 partial pressure and 0.1 M of added sulphate at 150 A m^{-2}. On the other hand, Almajed *et al.*[39] reported that better efficiencies of the electrolytic cell could be ensured by an optimal combination of carbonates and bicarbonates in the effluent.

The BPMED system for DAC, integrated into an absorption column, was firstly investigated by Sabatino *et al.*,[20] who developed a mathematical model in MATLAB to estimate energy needs and costs of 236 kJ $mol_{CO_2}^{-1}$ and \$773 per ton_{CO_2}, respectively (more than 3 times higher than the cost estimated by carbon engineering for their absorption and thermal regeneration process). The same researchers reported that the membrane is the most limiting factor for cost so that cheaper membranes with better performance could reduce total costs below \$250 per ton_{CO_2}.[20] Better energetic performances can be obtained either with 100% K^+ selectivity for the cation exchange membrane or CO_2 absorption ratio leading to an energy demand of 154 kJ $mol_{CO_2}^{-1}$.[40] These results show that the improvement of K^+ selectivity in the cell and optimization of the air contactor to have higher CO_2 absorption ratios are interesting areas to investigate. Regarding the cost, Young *et al.*[41] carried out an economic analysis, finding a range of \$100–600 per ton_{CO_2} by 2050; therefore, strong policies are needed to minimize the overall costs and help the spread of such technologies.

The above literature review indicates that comprehensive techno-economic analyses of alternative e-DAC technologies are missing in the literature, along with environmental studies. Most of the previous reports are about the evaluation of technical feasibility and energy efficiency through experimental analyses without a direct comparison of several solutions in terms of cost and environmental burden. Environmental estimations have not been done so far. This work aims to fill these gaps: both costs and environmental burden are evaluated for BPMED, electrolysis, PCET, and ESA technologies, considering a scale-up through an innovative method such as the hybrid learning curve method.[41] Moreover, as an additional point of view, the most sustainable e-DAC solution is suggested according to the geographic location, exploited energy source, and time. The study has located these processes in three different geographic areas, namely, the US, Europe, and China, the regions with the highest CO_2 emissions around the world, exploiting different renewable and low-carbon energy sources (nuclear, wind, and solar), and in different periods (2023, 2030, 2050). The technique for the order of preference by similarity to an ideal solution (TOPSIS) is then applied to suggest the most sustainable e-DAC process over time, energy source, and geographic location.

2 Mathematical modelling

A workflow diagram to visually illustrate the computational methodology described in this section is presented in Fig. 1, and it is explained in detail in the following paragraphs.

2.1 Description of e-DAC technologies

The BPMED, electrolytic cell, PCET, and ESA technologies are the e-DAC systems considered herein. BPMED and electrolytic cells can also be considered as regeneration technologies, while ESA and PCET are mainly separation processes.

Fig. 2a shows the process scheme for the BPMED cell, as reported by Sabatino *et al.*[20,42] The single cell has an acidic and alkaline compartment separated by a cation exchange membrane (CEM) in addition to a bipolar membrane for water dissociation. The acidic side is fed by a rich solution of carbonates and bicarbonates coming from the DAC absorption column. Here, the influx of protons (H^+) produced by the electro-dissociation of water inside the bipolar membrane reduces the pH, converting the carbonate ions into dissolved carbon dioxide. At the same time, K^+ ions are transported across the CEM to the alkaline compartment. The CO_2 in the gas phase is finally recovered in a knockout vessel from which the liquid stream that is depleted in KOH and CO_2 is fed to the alkaline compartment, where it receives the influx of K^+ from the acidic compartment and OH^- from the bipolar membrane. The alkaline hydroxide solution (KOH) is then regenerated and can be recycled to the absorption column.

As described by Almajed *et al.*[43] and in Fig. 2b, the rich CO_2 solution coming from the absorption column (K_2CO_3–$KHCO_3$

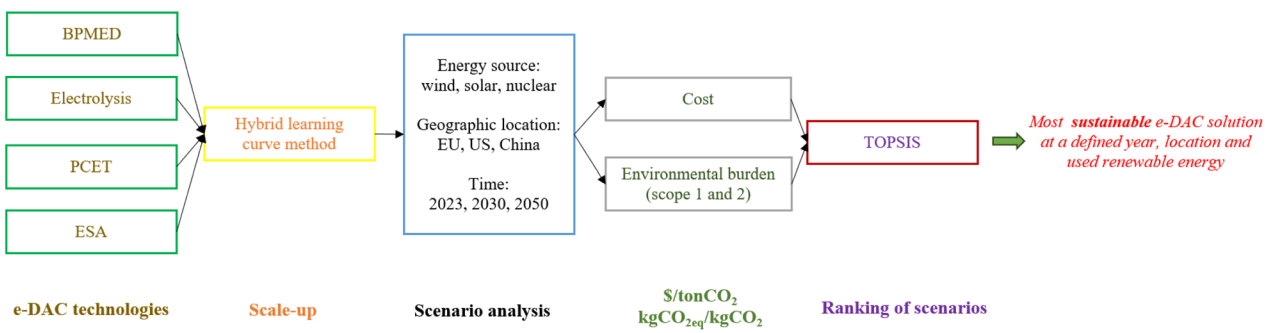

Fig. 1 Workflow diagram of the used computational methodology.

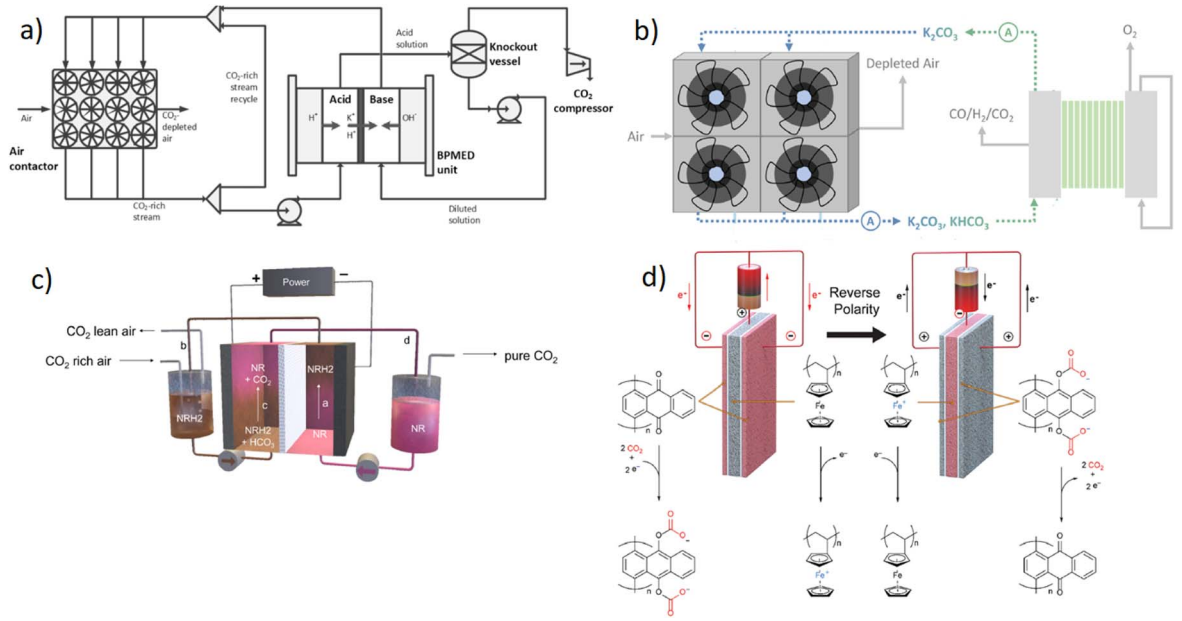

Fig. 2 Scheme of the operating principle of e-DAC technologies: (a) BPMED, (b) electrolysis, (c) PCET, and (d) ESA.[20,29,34,43]

mixed water solution) is fed into the acidic chamber, where the lower pH leads to the dissociation of the solution, resulting in CO_2 release in gaseous form. The CO_2 is reduced electrochemically to form carbon monoxide (CO) and carbonates (CO_3^{2-}) using the dissolved HCO^{3-}. The obtained solution is then neutralized by protons, K^+, and H^+ (coming from the anode side through the CEM) to reproduce the capturing solvent (K_2CO_3 aqueous solution) sent to the absorption column. Oxygen (O_2) is also co-generated at the anode side following the water oxidation reaction, while hydrogen (H_2) is co-produced at the cathode side according to the reduction reaction.

A continuous flow electrochemical system using neutral red (NR)/leuco-neutral red (NRH_2) as the redox active material in aqueous solution is considered for the PCET technology as reported by Seo *et al.*[34] and in Fig. 2c. In the process, NR is reduced electrochemically to provide NRH_2 with an increase in the pH of the solution (path a). The basic aqueous solution is pumped to the reservoir, where the air is introduced (path b). The CO_2-saturated solution is then pumped to the anodic chamber, where the electrochemical oxidation leads to the regeneration of NR and release of free CO_2 (path c). The resulting solution is then transferred to the anolyte reservoir to discharge CO_2 and close the flow cycle (path d).

The ESA technology considered here is that described by Voskian and Hatton[29] and its electro-swing cell is composed of two quinone electrodes (quinone-carbon nanotube (Q-CNT) as cathodes) sandwiching a single ferrocene electrode (ferrocene-CNT (Fc-CNT) as the anode) isolated from them by electrolyte membrane separators to prevent short circuits, as shown in Fig. 2d. The operating principle is as follows: the power source creates a voltage that causes electrons to flow from the ferrocene to the quinone through the wires. The quinone is then negatively charged, and when the air is blown through these electrodes, it captures the CO_2 until all the active sites on its surface are saturated. During the discharge cycle, the direction of the voltage on the cell is reversed; electrons flow from the quinone back to the ferrocene. The quinone is no longer negatively charged, so it has no chemical affinity for CO_2. The CO_2 molecules are released and swept out of the system by a stream of purge gas for subsequent use or disposal. The quinone is hence regenerated and ready to capture CO_2 again in another cycle.

A battery to store the renewable electrical energy and a fan to blow air inside the system (only for based separation techniques) are integrated and considered in each e-DAC process.

2.2 Techno-economic modelling with the hybrid learning curve methodology

The hybrid learning curve methodology proposed by Roussanaly *et al.*[44] and Young *et al.*[41] is applied in this study to evaluate costs because it is consistent with the cost trajectory of early-stage technologies and a low technology readiness level (TRL). It combines bottom-up engineering-economic studies used to estimate the cost of a first-of-a-kind (FOAK) plant starting from a defined lower TRL, with technological learning projections accounting for cost reductions due to innovation, learning by doing, learning by using, and economies of scale.[41] In particular, the method includes the bottom-up part with the top-down technological learning projection, evaluating respectively the FOAK cost and costs at higher scales with respective energy demand.

FOAK capital and operating costs are evaluated according to Young *et al.*[41] The FOAK capital cost is obtained by summing total engineering, procurement and construction (EPC) costs, process, and project contingency costs. Project contingency costs take into account costs not considered in the analysis due to the preliminary level of project specification, while process

contingency costs account for any uncertainty surrounding capital costs related to the technology maturity and cost of upscaling. EPC costs are provided by installed equipment costs with additional EPC costs (measured as the 15% of EPC costs). Table 1 provides the installed equipment costs of each e-DAC system (for ESA and PCET, the similarity of the lithium-ion battery and redox flow battery ZnBr is considered). The process contingency cost is a percentage of EPC costs according to the TRL value, fixed as in Table 1 (a linear correlation between TRL and percentage of EPC costs is obtained as reported by Young *et al.*[41]), while the project contingency is 35% of EPC costs.[41] To define the overall capital cost, the following costs are included in the FOAK CAPEX: owner's costs (7% of capital FOAK), spare parts (0.5% of capital FOAK), start-up capital (2% of capital FOAK), start-up labour (0.25 years of direct and indirect labour costs) and start up fuel/energy (0.02 years of fuel/energy costs).[41] At this stage, the capital cost of a battery ($1659 per kW) and fan ($200 per kW) are added to the calculation,[45,46] and for the annualization, a capital recovery factor (CRF) considering a lifetime of 20 years and a 10% of interest rate, is taken into account.

The operating FOAK cost is evaluated by summing the cost for energy consumption, direct labour (scaled linearly based on 278 employees at a 1 $Mton_{CO_2}$ per year plant), indirect labour (30% of direct labour and maintenance), maintenance (1.5% of capital FOAK), insurance (0.5% of capital FOAK) and local taxes and fees (0.5% of capital FOAK).[41]

Total costs are provided by the sum of overall capital costs and operating FOAK costs. The economic analysis is conducted for different geographic areas (China, the US, Europe), periods (2023, 2030, 2050), and energy sources (offshore wind, onshore wind, solar, nuclear), with prices provided in Table 2.[47]

Values of material scaling, productivity factor, and labour cost are reported for different geographic areas in Table S1 of the SI. In the top-down technological learning projection, capital costs and operating FOAK costs are extrapolated into higher scales using learning rates according to the following correlations (see eqn (1) and (2)):[41]

$$b = -\frac{\ln(1 - L_r)}{\ln(2)} \quad (1)$$

$$y = a \cdot x^{-b} \quad (2)$$

with b being the learning exponent, L_r the learning rate, y ($ per ton_{CO_2}) the new estimated total cost at the new capacity, a ($ per ton_{CO_2}) the total cost at FOAK conditions, and x the ratio between the new capacity and the initial capacity of the technology. In our calculations, for capital cost analysis, the learning rate value of BPMED and electrolysis processes is fixed to 14%,[41] while for ESA and PCET systems it is 6% and 4.5%, respectively.[46] For the operating FOAK cost, the learning rate is assumed to be 2.5% for all technologies.[41] On the other hand, the initial capacity of the technology (*e.g.* the FOAK scale) is that reported in the literature for which material and energy balances are provided: 45.6 $kton_{CO_2}$ per year for BPMED,[41] 0.08 ton_{CO_2} per year for PCET,[34] 646 ton_{CO_2} per year for electrolysis[43] and 2.2 $kton_{CO_2}$ per year for ESA.[29] The electrical energy demands for BPMED, PCET, electrolysis, and ESA are, respectively, 24 MJ $kg_{CO_2}^{-1}$, 65 kJ $mol_{CO_2}^{-1}$, 898 kW, and 90 kJ $mol_{CO_2}^{-1}$.[20,29,34,43]

Table 2 Prices of renewable electrical energy ($ per MWh) across different years and geographic areas[47]

	2023	2030	2050
Nuclear			
China	65	65	65
US	105	105	105
Europe	160	130	125
Solar			
China	50	30	20
US	50	30	25
Europe	65	40	30
Off-shore wind			
China	100	55	35
US	120	65	45
Europe	75	45	30
On-shore wind			
China	45	40	35
US	30	30	25
Europe	75	45	30

2.3 Environmental modelling

The environmental analysis is conducted according to scopes 1 and 2 because CO_2 emissions from electricity consumption and solvent usage are evaluated. For scope 2 CO_2 emissions, different emission factors are considered for electricity in the US, China, and Europe from different energy sources, as in Table 3.[41,48]

The top-down technological learning projection, as in eqn (1) and (2), with data related to operating conditions, is used to evaluate the energy and solvent consumption at higher scales of each investigated technology. For the solvent, a lifetime of 3 months is assumed.

Table 1 Installed equipment cost and TRL value for the investigated e-DAC technologies

	Installed equipment cost	Reference	TRL	Reference
BPMED	$31 M	Sabatino *et al.*[20,42]	4	Young *et al.*[41]
Electrolysis	$0.83 M	Almajed *et al.*[43]	3	Bouaboula *et al.*[19]
PCET	$3252 per kW	Mongird *et al.*[46]	2	Bouaboula *et al.*[19]
ESA	$1659 per kW	Mongird *et al.*[46]	1	Rosen *et al.*[58]

Table 3 Emission factors ($g_{CO_2\ eq}\ kWh^{-1}$) for different renewable energies and geographic areas

	EU	US	China
On-shore wind	5	5.84	8.6
Off-shore wind	7.8	7.28	25.5
Solar PV	31.8	55.9	60.1
Nuclear	7.2	12	7.6

In particular, a KOH water solution is used for the BPMED system in a base amount of 0.066 $ton_{KOH}\ ton_{CO_2}^{-1}$.[20,42] In the e-DAC technology based on electrolysis, a water solution of potassium carbonate (K_2CO_3) in a concentration of 1 M is used with a base amount of 0.03 $ton_{K2CO3}\ ton_{CO_2}^{-1}$.[43] For the PCET, the solvent in the system is composed of NR, nicotinamide (NA), and potassium chloride (KCl) in a base amount of 2.2×10^{-5} $ton_{NR}\ ton_{CO_2}^{-1}$, 0.00019 $ton_{NA}\ ton_{CO_2}^{-1}$, and 0.00011 $ton_{KCl}\ ton_{CO_2}^{-1}$, respectively.[34] No solvent consumption is taken into account in the ESA process due to its great stability after 7000 cycles. Emission factors of each solvent are taken from the Ecoinvent database and literature:[49,50] 2.15 $kg_{CO_2\ eq}\ kg^{-1}$ for KOH water solution, 2.42 $kg_{CO_2\ eq}\ kg^{-1}$ for the K_2CO_3 water solution, 101.5 $kg_{CO_2\ eq}\ kg^{-1}$ for NR, 0.595 $kg_{CO_2\ eq}\ kg^{-1}$ for KCl, and 10.8 $kg_{CO_2\ eq}\ kg^{-1}$ for NA.

2.4 TOPSIS modelling

TOPSIS analysis is one of the most used multi-criteria decision-making (MCDM) methods for analyzing, comparing, and ranking alternatives to choose the best and the most suitable option, considering the criteria of the problem.[51] For this method, the best alternative solution is that with the shortest Euclidean geometric distance from the positive ideal solution (PIS) and the longest Euclidean geometric distance from the negative ideal solution (NIS).

The TOPSIS analysis is conducted in this study, considering the following steps:[52]

Step 1: create an evaluation matrix $(x_{i,j})_{mxn}$ consisting of m alternatives and n criteria.

Step 2: the evaluation matrix $(x_{i,j})_{mxn}$ is normalized to form the matrix R, *e.g.*, $(r_{i,j})_{mxn}$, using the normalization method as in the following correlation (see eqn (3)):

$$r_{i,j} = \frac{x_{i,j}}{\sqrt{\sum_{k=1}^{m} {x_{k,j}}^2}} \quad i = 1, 2\ldots m,\ \ j = 1, 2, \ldots n \tag{3}$$

Step 3: calculate the weighted normalised decision matrix for which each element $t_{i,j}$ is provided by the multiplication between $(r_{i,j})_{mxn}$ and w_j. The last element w_j is the weight of each criterion evaluated in this work with the grey entropy method.

Step 4: determine the worst alternative (A_w) and the best alternative (A_b) (see eqn (4) and (5)):

$$A_w = \{<\max(t_{i,j}|i = 1, 2\ldots m)|j\in J_->, <\min(t_{i,j}|i = 1, 2\ldots m)|j\in J_+>\} \equiv \{t_{w,j}|j = 1, 2\ldots n\} \tag{4}$$

$$A_b = \{<\min(t_{i,j}|i = 1, 2\ldots m)|j\in J_->, <\max(t_{i,j}|i = 1, 2\ldots m)|j\in J_+>\} \equiv \{t_{b,j}|j = 1, 2\ldots n\} \tag{5}$$

where J^+ is associated with the criteria having a positive impact (TRL, amount of captured CO_2, potential for health and safety) and J^- is associated with the criteria having a negative impact (total costs and environmental burden).

Step 5: calculate the distance (d_{iw}) between the alternative target i and the worst condition A_w (see eqn (6)):

$$d_{iw} = \sqrt{\sum_{j=1}^{n} \left(t_{i,j} - t_{w,j}\right)^2} \quad i = 1, 2\ldots m \tag{6}$$

Calculate the distance (d_{ib}) between the alternative target i and the best condition A_b (see eqn (7)):

$$d_{ib} = \sqrt{\sum_{j=1}^{n} \left(t_{i,j} - t_{b,j}\right)^2} \quad i = 1, 2\ldots m \tag{7}$$

Step 6: calculate the similarity to the worst condition (see eqn (8)):

$$s_{iw} = \frac{d_{iw}}{d_{iw} + d_{ib}} \quad i = 1, 2\ldots m \tag{8}$$

Step 7: rank the alternatives according to s_{iw}

The entropy weighting method is an objective weighting technique that can calculate the relative importance among all criteria by comparing the entropy value for each criterion. However, for weighting analysis, a traditional entropy method based on the continuous type of entropy is not suitable for problems with discrete data. For this reason, Wen *et al.*[53] proposed the grey entropy based on the discrete type of entropy to properly conduct weighting analysis. The grey system theory is a good methodology that is used to solve uncertainty problems with discrete data and for problems where the information is limited, incomplete, and characterized by random uncertainty. The procedure for the grey entropy weighting includes the following steps:[54]

Step 1: calculate the summation of each criterion, D_j (see eqn (9)):

$$D_j = \sum_{i=1}^{m} x_{i,j} \quad j = 1, 2\ldots n \tag{9}$$

Step 2: calculate the normalization coefficient K (see eqn (10)):

$$K = \frac{1}{(e^{0.5} - 1)\cdot n} \tag{10}$$

with n being the total number of criteria.

Step 3: find the entropy for the specific criteria, e_j (see eqn (11)):

$$e_j = K\cdot \sum_{i=1}^{m} W_e(z_i) \quad j = 1, 2\ldots n \tag{11}$$

$$W_e(z_i) = z_i e^{(1-z_i)} + (1 - z_i)e^{z_i} - 1 \quad (12)$$

$$z_i = \frac{x_{i,j}}{D_j} \quad i = 1, 2\ldots m \quad (13)$$

Step 4: compute the total entropy value E (see eqn (14)):

$$E = \sum_{j=1}^{n} e_j \quad (14)$$

Step 5: determine the relative weighting factor λ_j (see eqn (15)):

$$\lambda_j = \frac{1}{n - E} \cdot (1 - e_j) \quad j = 1, 2\ldots n \quad (15)$$

Step 6: calculate the normalized weight of each criterion (see eqn (16)):

$$\beta_j = \frac{\lambda_j}{\sum_{j=1}^{n} \lambda_j} \quad j = 1, 2\ldots n \quad (16)$$

Alternatives considered in this analysis are the e-DAC technologies in different geographic areas around the world, using several energy sources and in different years. Moreover, the TOPSIS analysis is conducted considering five criteria: total costs, lifecycle environmental burden in terms of $kg_{CO_2\ eq}$ per kg of CO_2 captured, the amount of captured CO_2, TRL, and the potential for health and safety, with the aim to suggest the most sustainable e-DAC process. Economic criteria (total costs), technical criteria (TRL and amount of captured CO_2), environmental criteria (environmental impact), and social criteria (potential for health and safety) are taken into account for a sustainability evaluation.[55] Total costs, $kg_{CO_2\ eq}\ kg_{CO_2}^{-1}$, and the amount of captured CO_2 are those evaluated in our work, TRL is fixed according in Table 1, while the potential for health and safety data from Our World in Data[56] are considered for different energy sources (wind, nuclear and solar energies) and not for different technologies because they have the same objective (*e.g.* CO_2 capture from the air).

A sensitivity analysis considering the Monte Carlo simulation is carried out to simulate the variability in weights, so that the new weight (W_j) is according to the following equation (see eqn (17)):[57]

$$W_j = \frac{\theta_j \cdot \beta_j}{\sum_{i=1}^{n} \theta_i \cdot \beta_j} \quad j = 1, 2\ldots n \quad (17)$$

where θ_j, the aggregator, is obtained from a random uniform distribution with a percentage variation of basic weights (1000 sampling data).

3 Results and discussion

3.1 Results of economic analysis

In this section, results from the economic analysis are reported for each investigated region (the US, China, and Europe). Overall, it is possible to see that for all areas, energy sources, and years, e-DAC processes based on the electrolytic cell and BPMED have higher costs compared to other technologies due to the additional cost of the absorption column. ESA and PCET, both characterized by a simpler process, have lower costs. Regarding the range of total costs of e-DAC systems for each geographic region, in the US, the maximum value of the CO_2 capture cost at 1 $Mton_{CO_2}$ per year is \$1241 per ton_{CO_2} (for electricity driven by wind energy in the electrolysis process) while the minimum value is \$70 per ton_{CO_2} (for PCET driven by wind energy). In China, the highest total cost for capturing 1 $MtonCO_2$ per year, from the air is \$1027 per ton_{CO_2}, while the lowest value is 48 \$ per ton_{CO_2} for the electrolysis-based process and PCET, both fed by electricity from wind energy. On the other hand, in the EU, the range of capturing 1 $Mton_{CO_2}$ per year is between 1603 \$ per ton_{CO_2} and 78 \$ per ton_{CO_2} for an electrolysis process using nuclear energy and for PCET using onshore wind energy. There is little data in the literature about the cost analysis of e-DAC processes, so an easy comparison is not possible. However, it is reported that ESA should ultimately cost 50–100 \$ per ton_{CO_2},[59] in line with the results in this research, while for the BPMED-based process, Young *et al.*[41] reported costs up to 1000 \$ per ton_{CO_2}, as in our study.

3.1.1 Results for the US region. Fig. 3 shows the total cost of e-DAC technologies for the US with different energy sources for 2023. The total cost has a decreasing trend with the scale of the plant. Moreover, the use of an electrolytic cell integrated into an absorption column has the highest cost, followed by the BPMED, ESA, and PCET processes. For a plant capturing 1 $Mton_{CO_2}$ per year, considering nuclear energy (Fig. 3a), the capturing systems based on electrolysis, BPMED, ESA, and PCET cost 1112 \$ per ton_{CO_2}, 860 \$ per ton_{CO_2}, 123 \$ per ton_{CO_2}, and 84 \$ per ton_{CO_2}, respectively. When solar energy is used (Fig. 3b) to capture 1 $Mton_{CO_2}$ per year, the capturing process based on electrolysis, BPMED, ESA, and PCET has a total cost of 642 \$ per ton_{CO_2}, 537 \$ per ton_{CO_2}, 98 \$ per ton_{CO_2}, and 71 \$ per ton_{CO_2}, respectively. On the other hand, for capturing systems using onshore wind energy (Fig. 3c), the electrolysis-based process costs 470 \$ per ton_{CO_2}, that based on BPMED costs 417 \$ per ton_{CO_2}, ESA costs 88 \$ per ton_{CO_2}, while PCET has a cost of 67 \$ per ton_{CO_2}, when 1 $Mton_{CO_2}$ per year is captured from the air. Other solutions are found when offshore wind is used (Fig. 3d); the electrolysis-based process, BPMED-based process, ESA, and PCET cost 1241 \$ per ton_{CO_2}, 955 \$ per ton_{CO_2}, 130 \$ per ton_{CO_2}, and 52 \$ per ton_{CO_2}, respectively, when 1 $Mton_{CO_2}$ per year is removed from the atmosphere.

Fig. 4 presents data on the total costs of e-DAC processes for the US location from different energy sources for the year 2030. Considering the capture of 1 $Mton_{CO_2}$ per year, the most expensive system is that based on electrolysis, while the PCET system is the cheapest one for all energy sources. When nuclear energy is used, the electrolysis-based process, BPMED-based process, ESA, and PCET cost 1100 \$ per ton_{CO_2}, 862 \$ per ton_{CO_2}, 122 \$ per ton_{CO_2}, and 84 \$ per ton_{CO_2}, respectively (Fig. 4a). When solar energy is exploited, the total capture cost of processes using electrolysis, BPMED, ESA, and PCET is 469 \$ per ton_{CO_2}, 416 \$ per ton_{CO_2}, 88 \$ per ton_{CO_2}, and 67 \$ per ton_{CO_2},

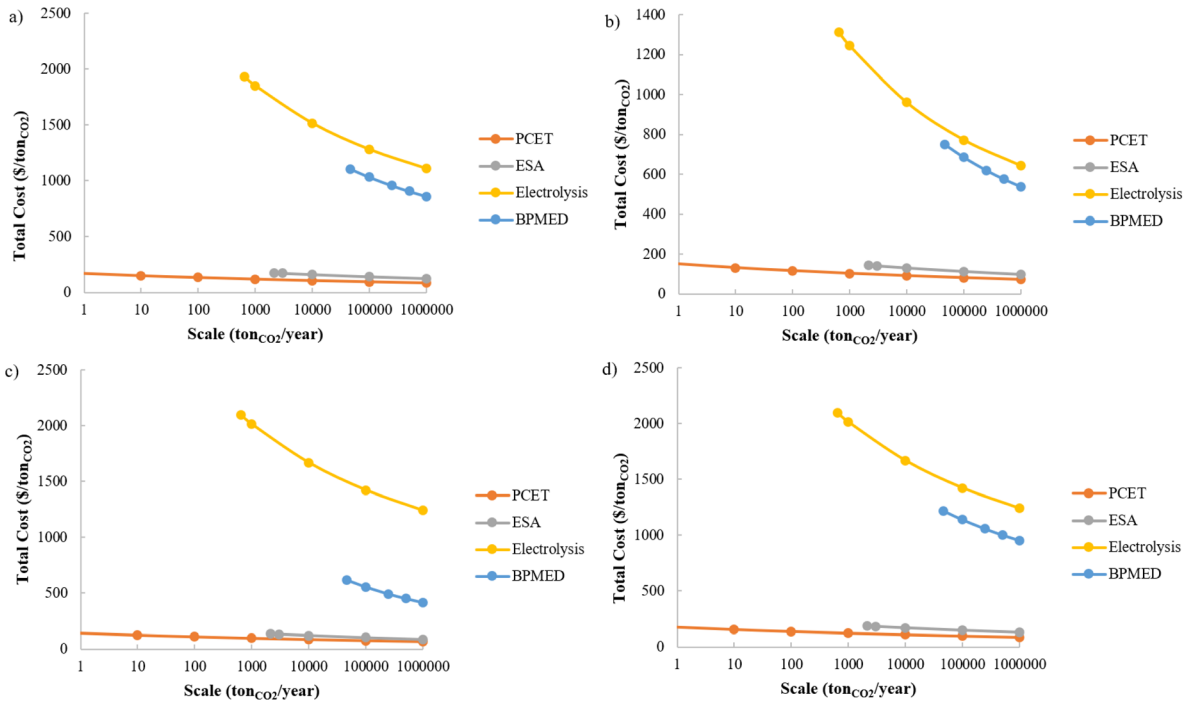

Fig. 3 Total costs of e-DAC technologies located in the US region for the year 2023 when (a) nuclear, (b) solar, (c) on-shore wind, and (d) off-shore wind energies are used.

respectively (Fig. 4b). On-shore wind is also considered in the analysis, and in this case, for the same capture capacity, the electrolysis-based process costs 469 $ per ton$_{CO_2}$, BPMED costs 416 $ per ton$_{CO_2}$, ESA has a total cost of 88 $ per ton$_{CO_2}$, while the cheapest one (*e.g.* PCET) costs 67 $ per ton$_{CO_2}$ (Fig. 4c). Fig. 4d shows the results for using off-shore wind energy at 1 Mton$_{CO_2}$

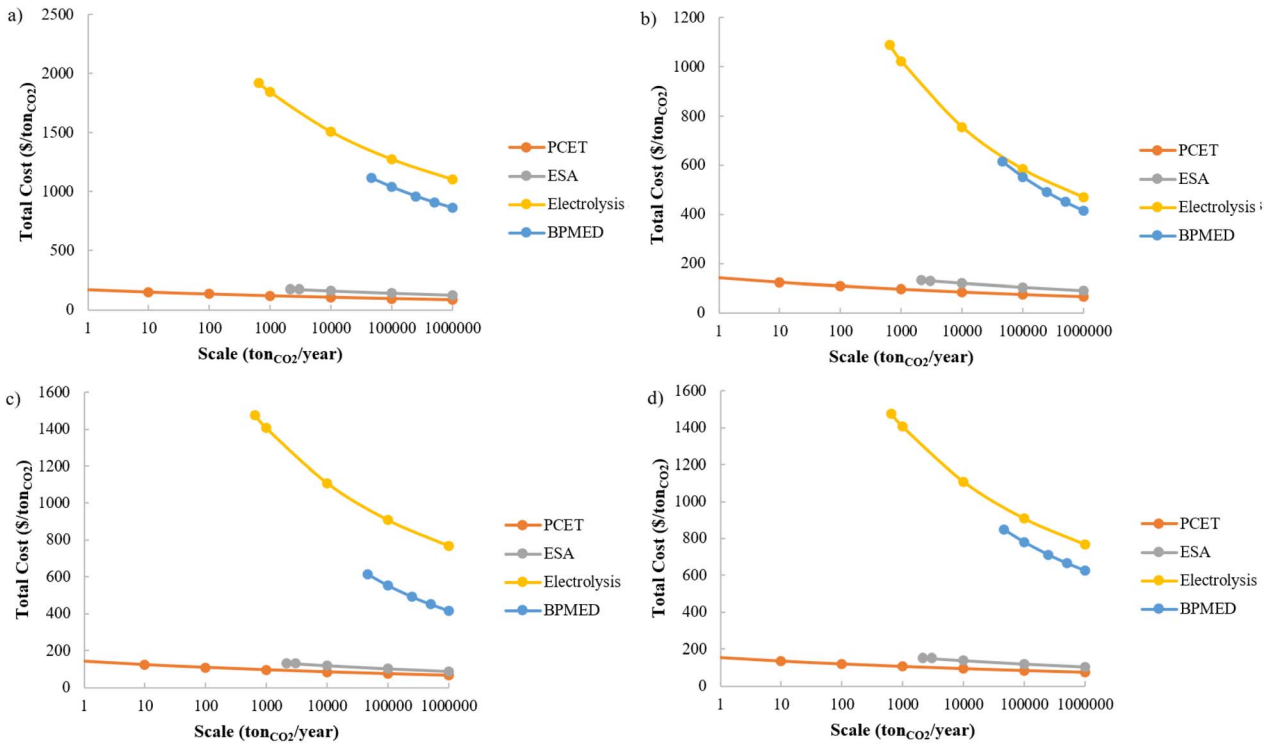

Fig. 4 Total costs of e-DAC technologies located in the US region for the year 2030 when (a) nuclear, (b) solar, (c) on-shore wind, and (d) off-shore wind energies are used.

per year; electrolysis, BPMED, ESA, and PCET cost 767 $ per ton_{CO_2}, 624 $ per ton_{CO_2}, 104 $ per ton_{CO_2}, and 75 $ per ton_{CO_2}, respectively.

In Fig. 5 total costs of e-DAC systems as a function of the plant scale are reported for the US for 2050. When nuclear energy is used, the cost of the electrolysis-based process, BPMED-based process, ESA, and PCET are, respectively, 1107 $ per ton_{CO_2}, 862 $ per ton_{CO_2}, 122 $ per ton_{CO_2}, and 84 $ per ton_{CO_2} for a capture capacity of 1 $MtonCO_2$ per year (Fig. 5a). For the same capacity, the use of solar energy causes a capture cost of 426 $ per ton_{CO_2}, 386 $ per ton_{CO_2}, 86 $ per ton_{CO_2}, and 66 $ per ton_{CO_2}, respectively, using electrolysis, BPMED, ESA, and PCET (Fig. 5b). Fig. 5c shows that the capture of 1 $Mton_{CO_2}$ per year using on-shore wind energy costs 426 $ per ton_{CO_2}, 386 $ per ton_{CO_2}, 86 $ per ton_{CO_2}, and 66 $ per ton_{CO_2} for electrolysis, BPMED, ESA, and PCET processes, respectively. On the other hand, when electricity from off-shore wind is supplied, 1 $Mton_{CO_2}$ per year of capture costs are respectively of 505 $ per ton_{CO_2}, 596 $ per ton_{CO_2}, 95 $ per ton_{CO_2}, and 70 $ per ton_{CO_2} for electrolysis, BPMED, ESA, and PCET processes, respectively (Fig. 5d).

3.1.2 Results for China. The total costs of capturing e-DAC systems are shown in Fig. 6 for China in 2023. In particular, Fig. 6a, reports results when the electricity is supplied by nuclear energy, and we can see that for a capacity of 1 $Mton_{CO_2}$ per year, the electrolysis-based process, BPMED-based process, ESA, and PCET cost, respectively, 715 $ per ton_{CO_2}, 568 $ per ton_{CO_2}, 81 $ per ton_{CO_2} and 55 $ per ton_{CO_2}. For the same capture capacity, the use of solar energy leads to a total cost of 587 $ per ton_{CO_2}, 482 $ per ton_{CO_2}, 74 $ per ton_{CO_2}, and 52 $ per ton_{CO_2}, respectively, for the processes based on electrolysis, BPMED, ESA, and PCET (Fig. 6b). On the other hand, supplying electricity with on-shore wind leads to a capture cost of 565 $ per ton_{CO_2} for the electrolysis-based process, 452 $ per ton_{CO_2} for the BPMED process, 72 $ per ton_{CO_2} for ESA, and 50 $ per ton_{CO_2} for PCET, at a scale of 1 $Mton_{CO_2}$ per year (Fig. 6c). Fig. 6d shows that capturing 1 $Mton_{CO_2}$ per year costs 1027 $ per ton_{CO_2} for the electrolysis-based process, 781 $ per ton_{CO_2} for the BPMED-based process, 75 $ per ton_{CO_2} for ESA, and 63 $ per ton_{CO_2} for PCET.

Fig. 7 reports the capture cost in China for the year 2030. When the electricity is driven by nuclear energy (Fig. 7a), the most expensive e-DAC process is based on electrolysis: for a scale of 1 $Mton_{CO_2}$ per year, it costs 712 $ per ton_{CO_2}. The cheapest one (PCET) has a price of 55 $ per ton_{CO_2} to capture 1 $Mton_{CO_2}$ per year. ESA and PCET cost, respectively, 81 $ per ton_{CO_2} and 55 $ per ton_{CO_2}, at the same scale. In Fig. 7b, the processes driven by solar energy are reported: to capture 1 $Mton_{CO_2}$ per year, the electrolysis-based process, BPMED process, ESA, and PCET cost, respectively, 414 $ per ton_{CO_2}, 362 $ per ton_{CO_2}, 65 $ per ton_{CO_2} and 47 $ per ton_{CO_2}. Results for the use of on-shore wind for electricity generation are reported in Fig. 7c. Here, for a capture capacity of 1 $Mton_{CO_2}$ per year, the electrolysis-based system, BPMED, ESA, and PCET have respective prices of 499 $ per ton_{CO_2}, 421 $ per ton_{CO_2}, 70 $ per ton_{CO_2}, and 49 $ per ton_{CO_2}. On the other hand, when electricity is supplied by off-shore wind energy, to capture 1 $Mton_{CO_2}$ per year, the e-DAC based on electrolytic cells costs

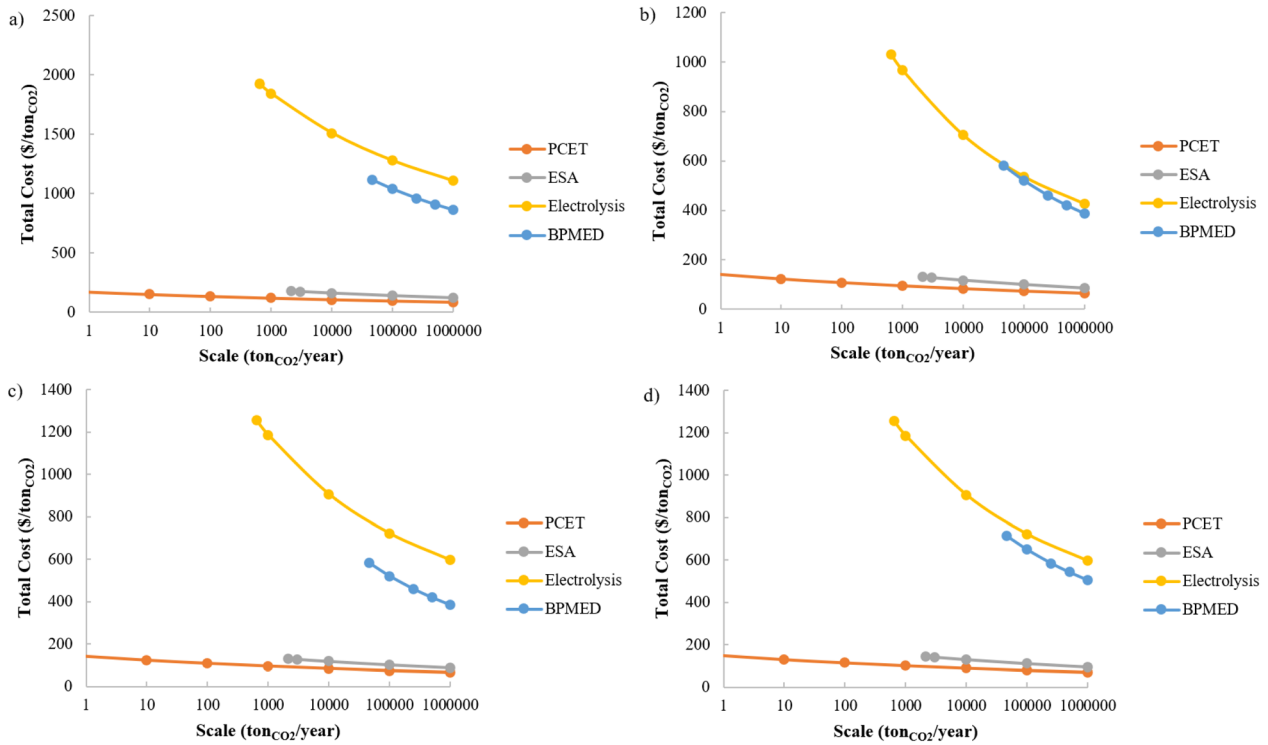

Fig. 5 Total costs of e-DAC technologies located in the US region for the year 2050 when (a) nuclear, (b) solar, (c) on-shore wind, and (d) off-shore wind energies are used.

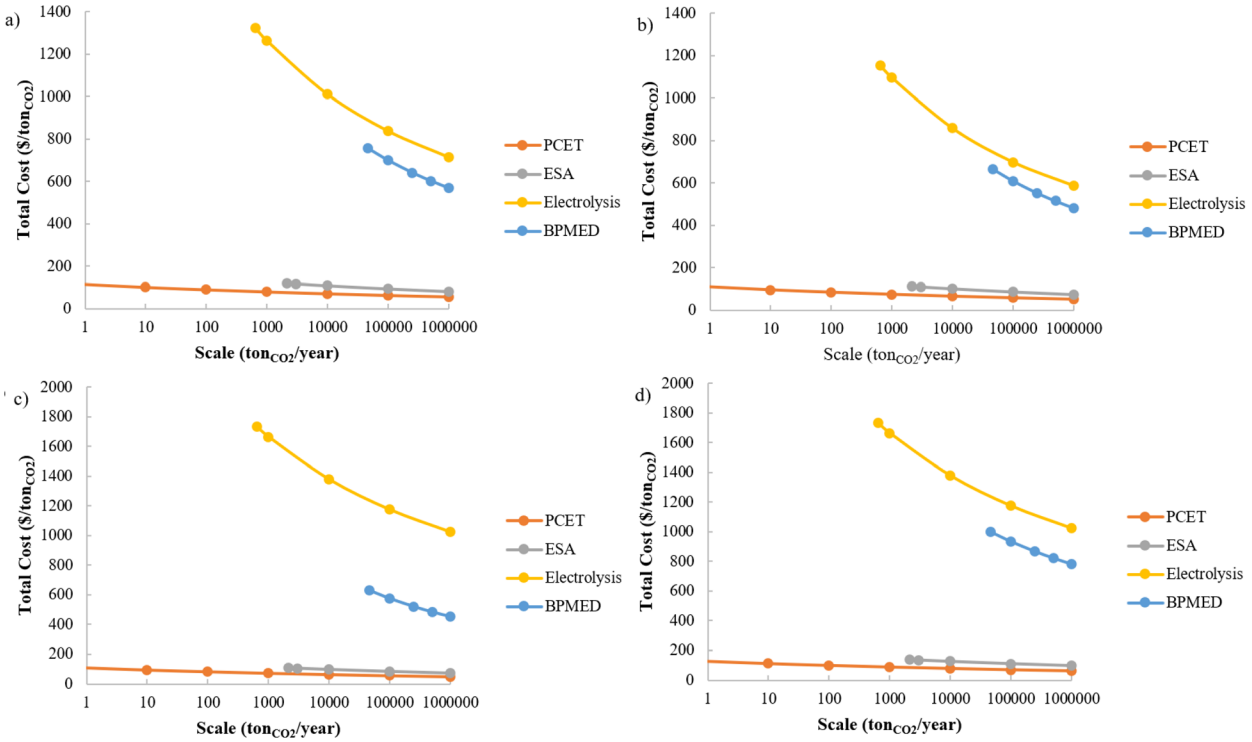

Fig. 6 Total costs of e-DAC technologies located in China for the year 2023 when (a) nuclear, (b) solar, (c) on-shore wind, and (d) off-shore wind energies are used.

627 \$ per ton$_{CO_2}$, that based on BPMED costs 510 \$ per ton$_{CO_2}$, while ESA and PCET have prices of 76 \$ per ton$_{CO_2}$ and 53 \$ per ton$_{CO_2}$ (Fig. 7d).

The economic analysis results for China in 2050 are reported in Fig. 8, where it is possible to see that when nuclear energy is exploited for electrical energy generation, for a scale of 1

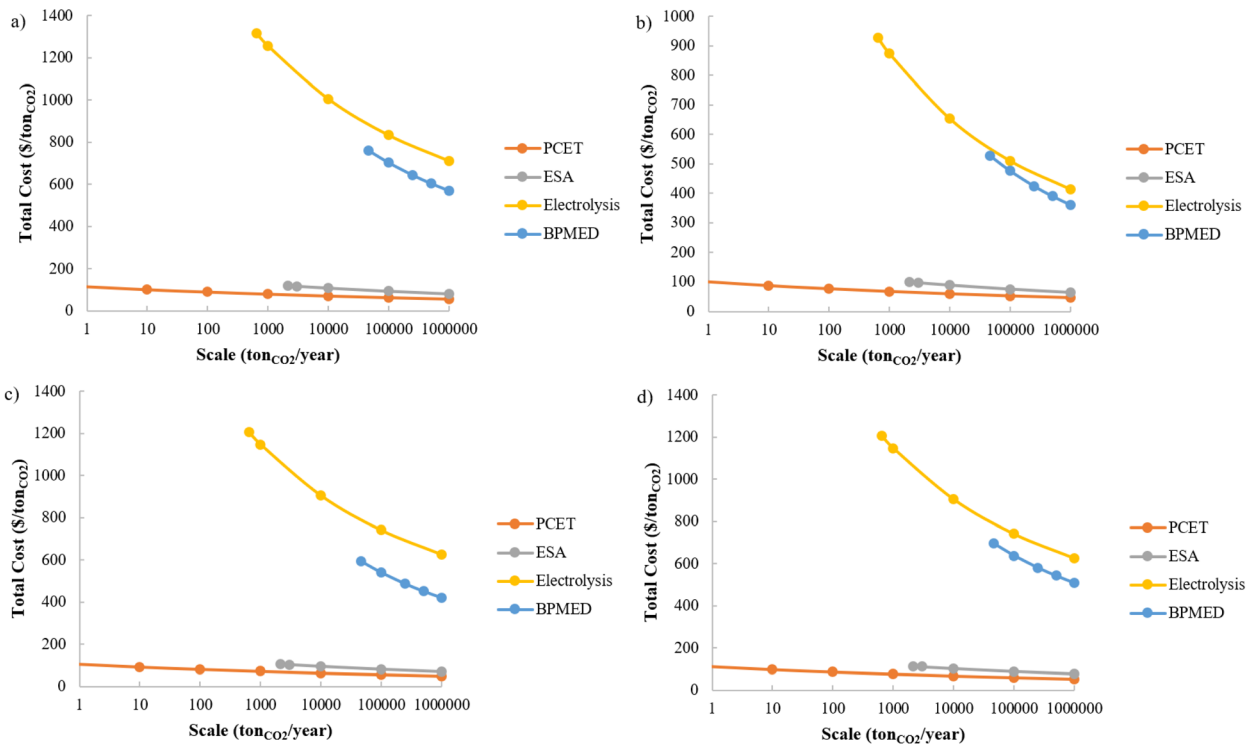

Fig. 7 Total costs of e-DAC technologies located in China for the year 2030 when (a) nuclear, (b) solar, (c) on-shore wind, and (d) off-shore wind energies are used.

Mton$_{CO_2}$ per year, the electrolysis-based process, BPMED-based process, ESA, and PCET cost, respectively, 712 $ per ton$_{CO_2}$, 570 $ per ton$_{CO_2}$, 81 $ per ton$_{CO_2}$ and 55 $ per ton$_{CO_2}$. In the solar energy case, for a capture capacity of 1 Mton$_{CO_2}$ per year, e-DAC systems using electrolysis, BPMED, ESA and PCET cost, respectively, 329 $ per ton$_{CO_2}$, 302 $ per ton$_{CO_2}$, 60 $ per ton$_{CO_2}$, and 45 $ per ton$_{CO_2}$ (Fig. 8b). Fig. 8c shows the results of capture costs when on-shore wind energy is used to produce electricity. For a capture capacity of 1 Mton$_{CO_2}$ per year, PCET, ESA, BPMED, and electrolysis systems cost, respectively, 48 $ per ton$_{CO_2}$, 67 $ per ton$_{CO_2}$, 391 $ per ton$_{CO_2}$, and 456 $ per ton$_{CO_2}$. On the other hand, the used of off-shore wind energy to produce electricity and to remove 1 Mton$_{CO_2}$ per year from the air, causes the following capture cost for the electrolysis, BPMED, ESA and PCET processes: 456 $ per ton$_{CO_2}$, 391 $ per ton$_{CO_2}$, 67 $ per ton$_{CO_2}$ and 48 $ per ton$_{CO_2}$ (Fig. 8d).

3.1.3 Results for the European region. Fig. 9 shows results from the economic analysis for the European region in 2023. The results for the use of nuclear energy are reported in Fig. 9a. Also in this case, the most expensive capture system is that based on electrolysis (1600 $ per ton$_{CO_2}$ to capture 1 Mton$_{CO_2}$ per year) while the PCET has the lowest cost (103 $ per ton$_{CO_2}$ to capture 1 Mton$_{CO_2}$ per year). ESA and BPMED cost, respectively, 155 $ per ton$_{CO_2}$ and 1207 $ per ton$_{CO_2}$ for a scale of 1 Mton$_{CO_2}$ per year. Fig. 9b shows costs as a function of the scale when electricity is driven by solar energy. To capture 1 Mton$_{CO_2}$ per year, electrolysis, BPMED, ESA, and PCET, respectively, have prices of 790 $ per ton$_{CO_2}$, 645 $ per ton$_{CO_2}$, 112 $ per ton$_{CO_2}$, and 81 $ per ton$_{CO_2}$. Results were also obtained for electricity generated by onshore and offshore wind, as shown in Fig. 9c and 8d, respectively. When on-shore wind is used to supply electricity, the electrolysis-based process, BPMED, ESA, and PCET, respectively, cost 768 $ per ton$_{CO_2}$, 616 $ per ton$_{CO_2}$, 110 $ per ton$_{CO_2}$, and 80 $ per ton$_{CO_2}$ at a scale of 1 Mton$_{CO_2}$ per year. On the other hand, for the off-shore wind case study, the electrolysis-based process, BPMED, ESA, and PCET cost 875 $ per ton$_{CO_2}$, 705 $ per ton$_{CO_2}$, 117 $ per ton$_{CO_2}$, and 84 $ per ton$_{CO_2}$ at a scale of 1 Mton$_{CO_2}$ per year (Fig. 9d).

Fig. 10 shows the total costs of e-DAC systems as a function of capture capacity for the European region in 2030. Results for the use of nuclear energy to generate electricity are shown in Fig. 10a, where 1 Mton$_{CO_2}$ per year capture costs are, respectively, 1340 $ per ton$_{CO_2}$, 1030 $ per ton$_{CO_2}$, 141 $ per ton$_{CO_2}$, and 96 $ per ton$_{CO_2}$ for the electrolysis-based process, BPMED, ESA, and PCET. When solar energy is exploited to produce electricity, the electrolysis-based process still has the highest capture cost (573 $ per ton$_{CO_2}$ for 1 Mton$_{CO_2}$ per year), while PCET has the lowest cost (76 $ per ton$_{CO_2}$ for 1 Mton$_{CO_2}$ per year) (Fig. 10b). ESA and BPMED cost 100 $ per ton$_{CO_2}$ and 494 $ per ton$_{CO_2}$, respectively, to capture 1 Mton$_{CO_2}$ per year. Electricity can be generated by on-shore wind energy, leading to a capture cost of 701 $ per ton$_{CO_2}$ for the electrolysis-based process, 584 $ per ton$_{CO_2}$ for the BPMED-based process, 107 $ per ton$_{CO_2}$ for the ESA, and 79 $ per ton$_{CO_2}$ for the PCET (Fig. 10c). On the other hand, the electrolysis, BPMED, ESA, and PCET processes cost, respectively, 616 $ per ton$_{CO_2}$, 524 $ per ton$_{CO_2}$, 103 $ per ton$_{CO_2}$, and 77 $ per ton$_{CO_2}$ when electricity generated by off-shore wind drives the overall system (Fig. 10d).

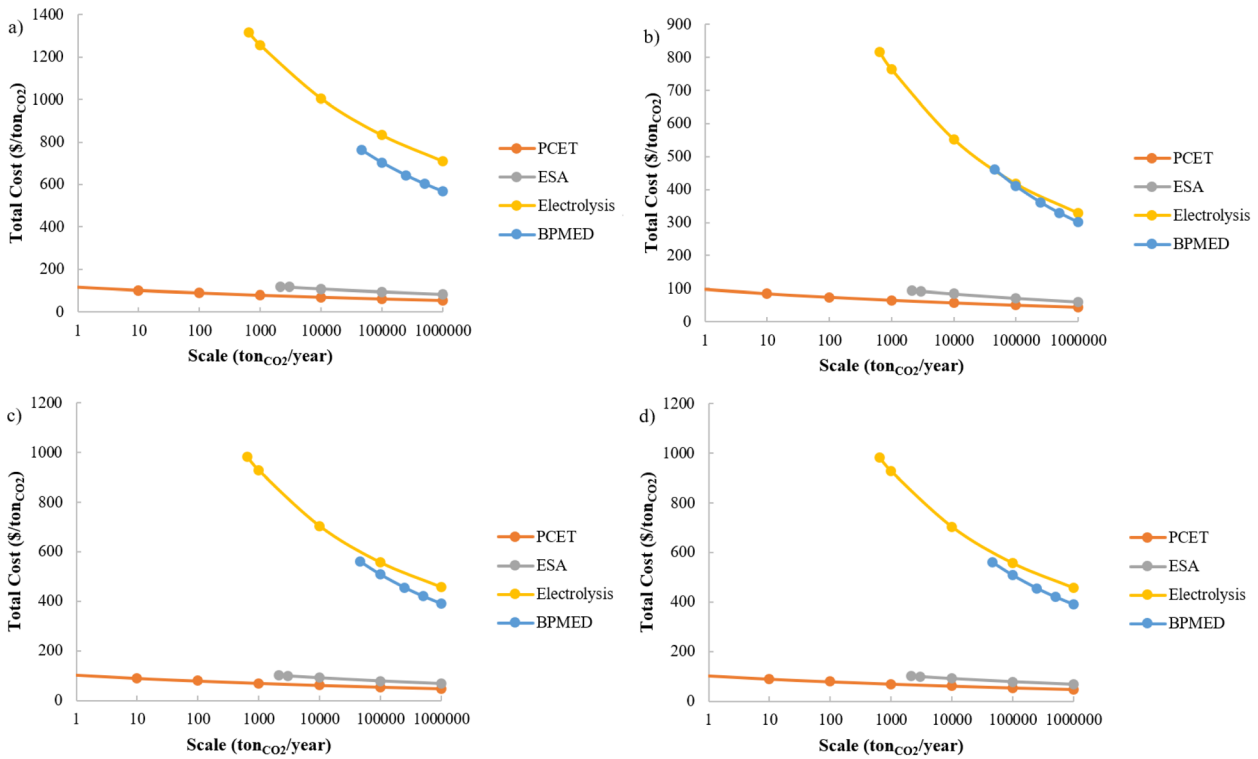

Fig. 8 Total costs of e-DAC technologies located in China for the year 2050 when (a) nuclear, (b) solar, (c) on-shore wind, and (d) off-shore wind energies are used.

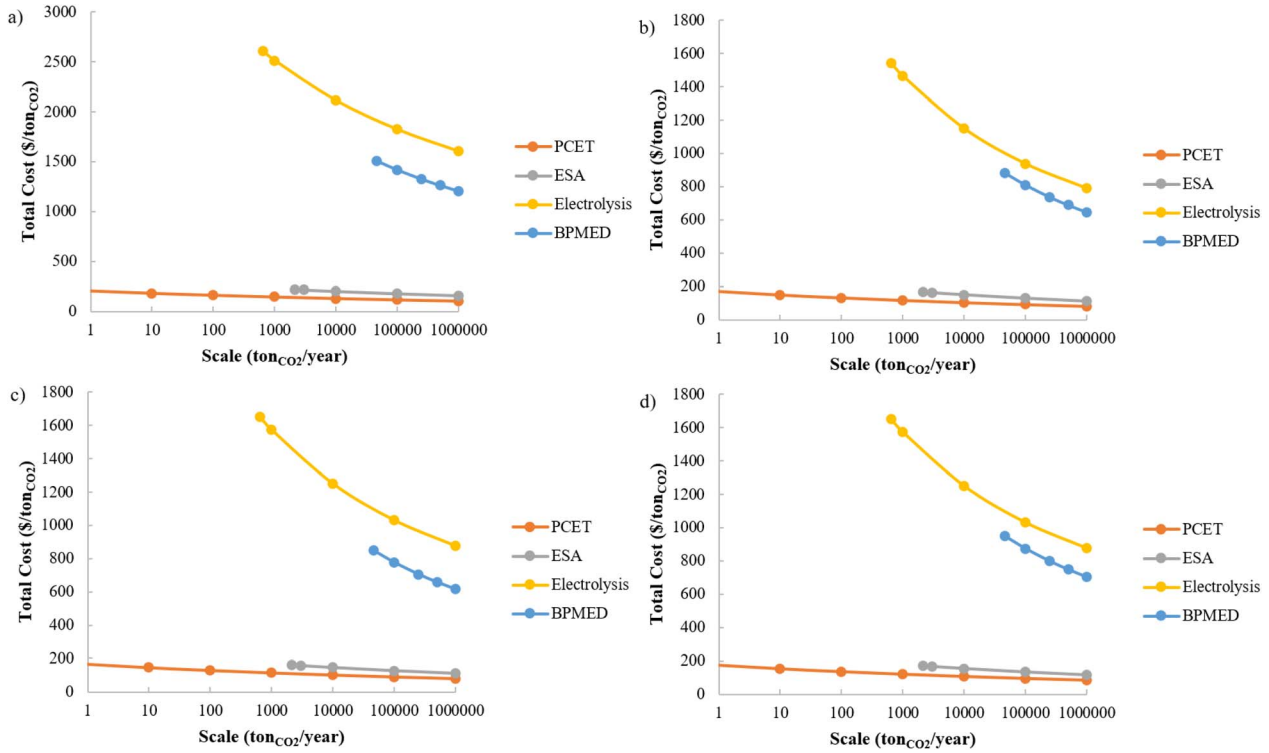

Fig. 9 Total costs of e-DAC technologies located in Europe for the year 2023 when (a) nuclear, (b) solar, (c) on-shore wind, and (d) off-shore wind energies are used.

Total capture costs as a function of the scale are reported in Fig. 11 for the European region in 2050. In this case study, the electrolysis-based process is the most expensive process only when nuclear, solar, and offshore wind energies are used, having a capture cost of 1296 \$ per ton$_{CO_2}$, 488 \$ per ton$_{CO_2}$, and 488 \$ per ton$_{CO_2}$, respectively, for a capture capacity of 1

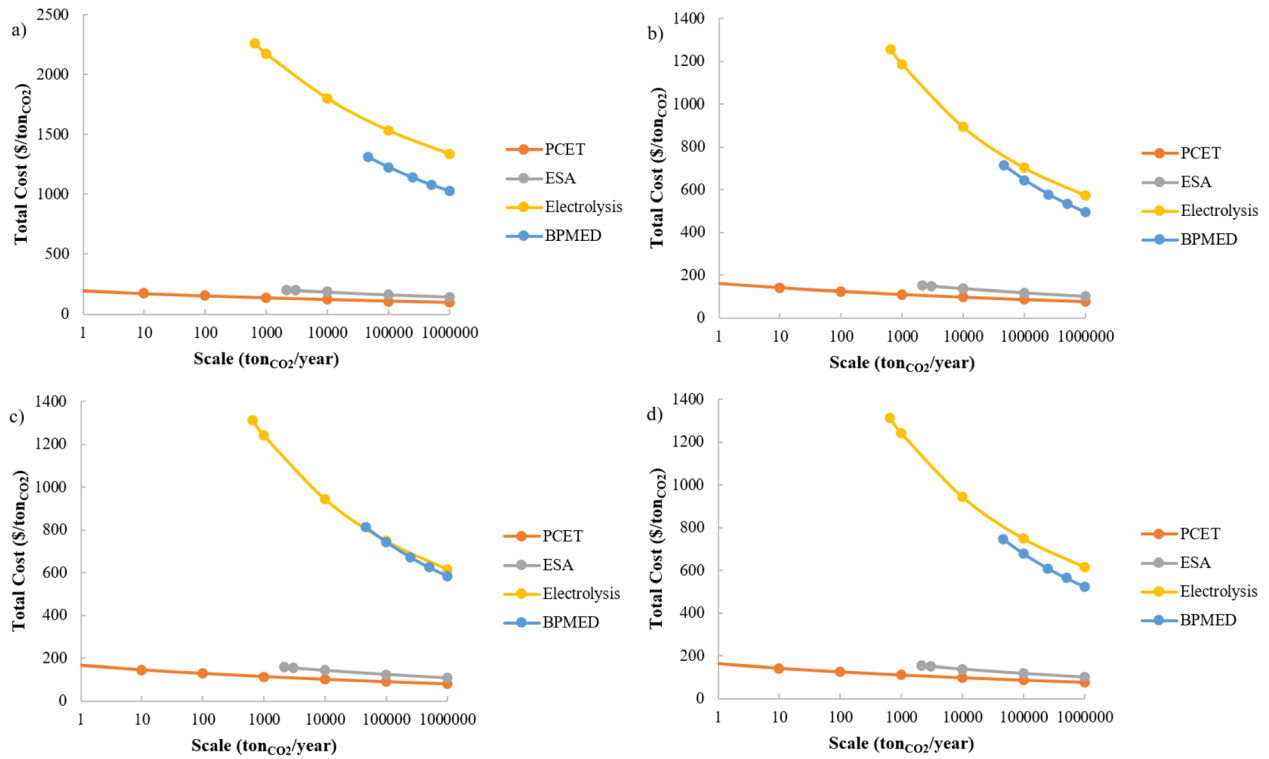

Fig. 10 Total costs of e-DAC technologies located in Europe for the year 2030 when (a) nuclear, (b) solar, (c) on-shore wind, and (d) off-shore wind energies are used.

$Mton_{CO_2}$ per year. When onshore wind energy is exploited to generate electricity, the most expensive process is the BPMED (it costs 554 $ per ton_{CO_2} for 1 Mt_{CO_2} per year). The PCET system always has the lowest cost to capture 1 $Mton_{CO_2}$ per year: 165 $ per ton_{CO_2}, 125 $ per ton_{CO_2}, 133 $ per ton_{CO_2}, and 88 $ per ton_{CO_2}, respectively, for using nuclear, solar, on-shore, and off-shore wind energies.

Higher costs are seen for the ESA process with 139 $ per ton_{CO_2}, 96 $ per ton_{CO_2}, 105 $ per ton_{CO_2}, and 96 $ per ton_{CO_2} in the case of using nuclear, solar, on-shore, and off-shore wind energies, respectively (capture capacity of 1 $Mton_{CO_2}$ per year). On the other hand, the BPMED process costs 1000 $ per ton_{CO_2} for exploiting nuclear energy, 435 $ per ton_{CO_2} for exploiting solar and offshore wind energies (capture capacity 1 $Mton_{CO_2}$ per year).

3.2 Results of the environmental analysis

The environmental analysis is conducted, evaluating the $kg_{CO_2\ eq}\ kg_{CO_2}^{-1}$ (*i.e.*, the unit of service is 1 kg CO_2 captured from the atmosphere) captured for different energy sources, geographic areas, and e-DAC technologies. CO_2 emissions from the use of electrical energy and solvents are measured and are independent of the year. Fig. 12 shows results for the US region for different energy sources (nuclear in Fig. 12a, solar in Fig. 12b, offshore wind in Fig. 12c, onshore wind in Fig. 12d), where the $kg_{CO_2\ eq}\ kg_{CO_2}^{-1}$ that is captured is a function of the plant scale. For all energy sources, a small variation of the environmental burden with the scale is present for ESA and PCET technologies due to a lower amount of CO_2 emitted compared to that captured. On the other hand, the electrolysis and BPMED-based processes have a higher variation of this parameter with the capture capacity of the plant because the capture efficiency is lower and about 50%.[20,42] Considering the capture of 1 $Mton_{CO_2}$ per year, the use of electricity from solar renewable energy sources causes the highest environmental impact ($-0.47\ kg_{CO_2\ eq}\ kg_{CO_2}^{-1}$ captured for the electrolysis-based process), while the electricity from on-shore wind energy causes the lowest environmental burden ($-0.995\ kg_{CO_2\ eq}\ kg_{CO_2}^{-1}$ captured for the PCET system). ESA and PCET have a lower environmental impact, while electrolysis and BPMED have a higher environmental burden, even though all are characterized by a negative value of the parameter related to the emitted CO_2.

Fig. 13 shows the results of the environmental analysis for China at different renewable energies (nuclear in Fig. 13a, solar in Fig. 13b, offshore wind in Fig. 13c, onshore wind in Fig. 13d). The trend of $kg_{CO_2\ eq}\ kg_{CO_2}^{-1}$ captured as a function of plant scale is analogous to the US case study, so the same considerations are valid. Also, in this case, solar energy causes the highest environmental impact ($-0.43\ kg_{CO_2\ eq}\ kg_{CO_2}^{-1}$ captured for the electrolysis-based process at 1 $Mton_{CO_2}$ per year capture capacity), while nuclear energy leads to the lowest environmental burden ($-0.995\ kg_{CO_2\ eq}\ kg_{CO_2}^{-1}$ captured for the PCET system at 1 $Mton_{CO_2}$ per year capture capacity).

Results for the environmental impact of e-DAC technologies are reported in Fig. 14 for the European region, showing a similar trend to China and US case studies due to the same reasons. In Fig. 14a, results are related to the use of nuclear energy; in Fig. 14b, results are related to the use of solar energy,

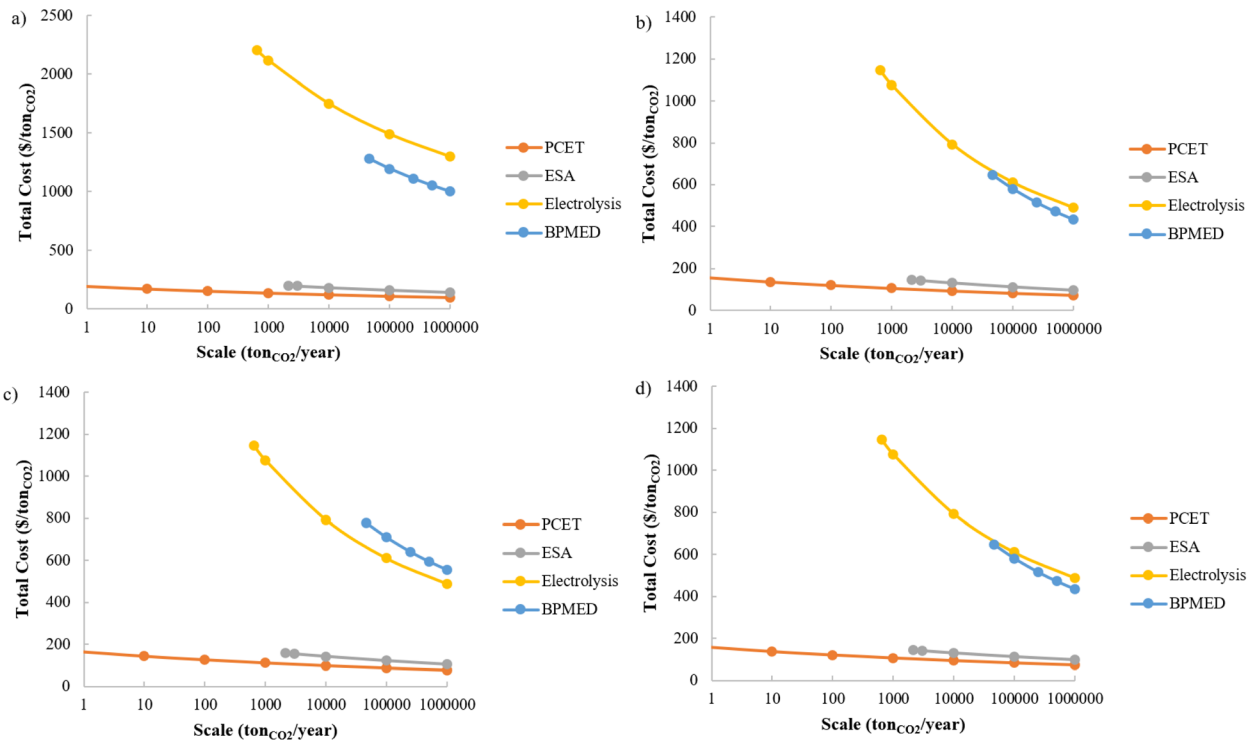

Fig. 11 Total costs of e-DAC technologies located in Europe for the year 2050 when (a) nuclear, (b) solar, (c) on-shore wind, and (d) off-shore wind energies are used.

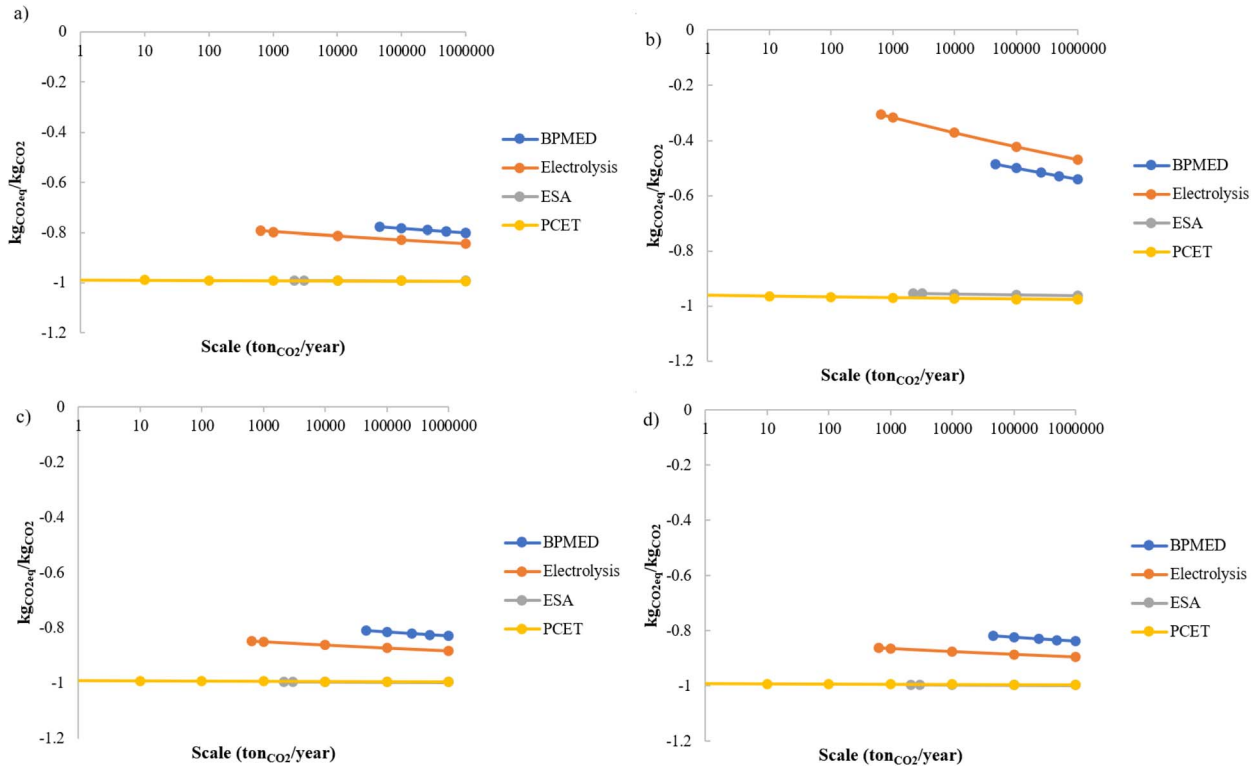

Fig. 12 Environmental burden of e-DAC technologies located in the US when (a) nuclear, (b) solar, (c) off-shore wind, and (d) on-shore wind energies are used.

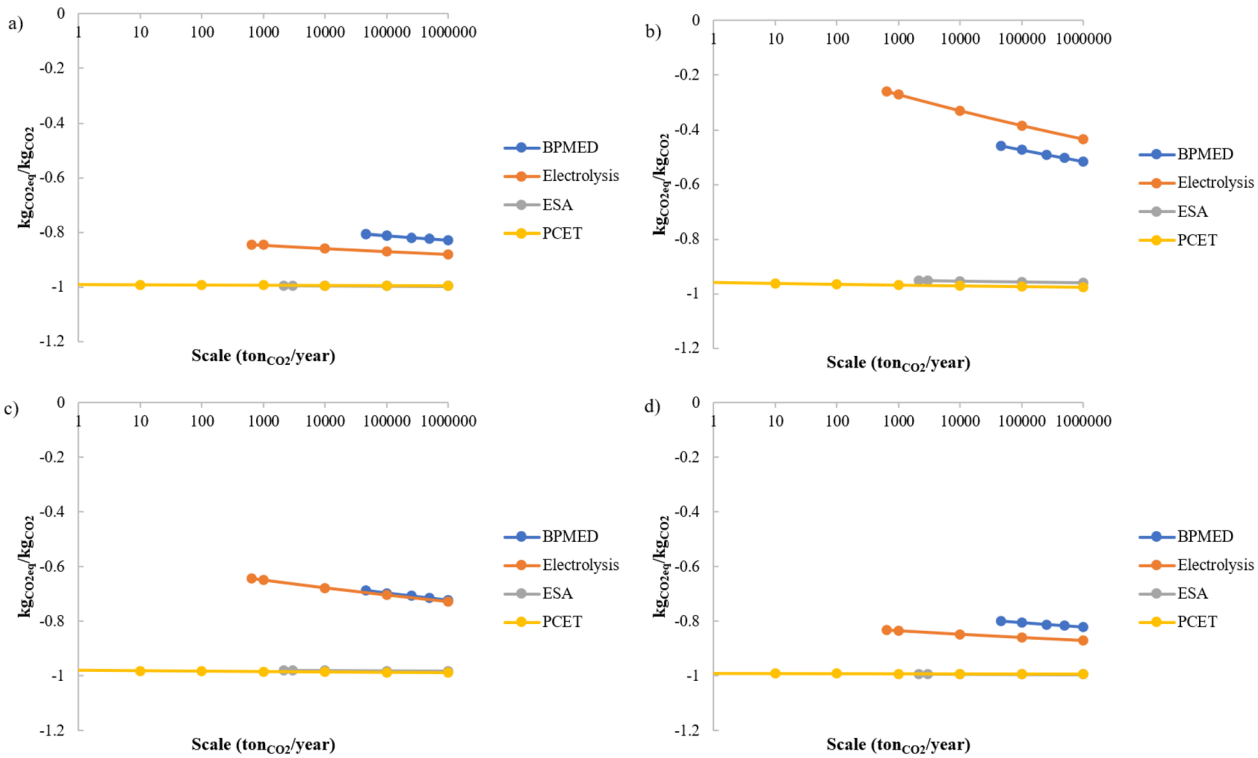

Fig. 13 Environmental burden of e-DAC technologies located in China when (a) nuclear, (b) solar, (c) off-shore wind, and (d) on-shore wind energies are used.

while Fig. 14c and d are related to off-shore and on-shore wind energies, respectively. For the European Union, electricity produced by solar energy still causes the highest environmental burden (-0.673 $kg_{CO_2\ eq}$ $kg_{CO_2}^{-1}$ captured for the electrolysis-based process at 1 $Mton_{CO_2}$ per year capture capacity), while electrical energy supplied by on-shore wind produces the lowest value of $kg_{CO_2\ eq}$ $kg_{CO_2}^{-1}$ captured for PCET at 1 $Mton_{CO_2}$ per year (-0.996 $kg_{CO_2\ eq}$ $kg_{CO_2}^{-1}$ captured).

A comparison with the literature is not possible because similar analyses have not yet been carried out for DAC technologies that are fully electrified. Overall, it is possible to see that for all regions around the world, ESA and PCET processes have a lower environmental impact while BPMED and electrolysis-based processes have a higher environmental impact, independent of the energy source.

3.3 Results of TOPSIS analysis

A TOPSIS analysis is conducted to rank the investigated alternatives among e-DAC technologies, considering the time, energy source, and geographic location simultaneously. The results are reported in Table 4 for the first 10 ranked and selected solutions, showing that PCET is the best technology considering economic, environmental, social, and technical aspects together. It is, therefore, considered a promising e-DAC process. From the above results, PCET also has lower costs and environmental impacts. However, several critical barriers must be addressed for successful deployment, particularly around material availability, system durability, and integration with renewable energy grids. PCET systems often rely on specialized redox-active molecules and catalysts, some of which have limitations in scalability (*e.g.*, scarcity of active materials, sustainable material sourcing, cost constraints). Operational lifetime is crucial for any e-DAC technology to be economically and environmentally viable due to electrochemical instability, membrane and separation degradation, thermal and mechanical cycling, and contamination from air. Moreover, PCET presents some specific challenges due to the intermittent power supply (must tolerate variable current and frequent cycling, which can accelerate degradation), dynamic operation, energy efficiency matching, and grid synchronization.

Inside this context, some solutions to the material availability can involve the development of stable, non-toxic, and earth-abundant redox mediators (*e.g.*, modified quinones, polyoxometalates, phenazines) or designing recyclable or self-healing electrodes and membranes. Regarding the system design, it would be useful to incorporate real-time sensors and AI control to manage degradation and optimize performance, as well as use modular, replaceable components to improve maintenance and extend system life. For the renewable compatibility, it is suggested to develop systems that can operate efficiently under pulsed or variable power input.

The results indicate that the best place to build a fully electrified DAC system is China, followed by the US. Moreover, today is not the best time to construct these kinds of technologies; the years 2040–2050 are, in fact, the preferred time due to an expected lower cost of electricity and hence operating costs.

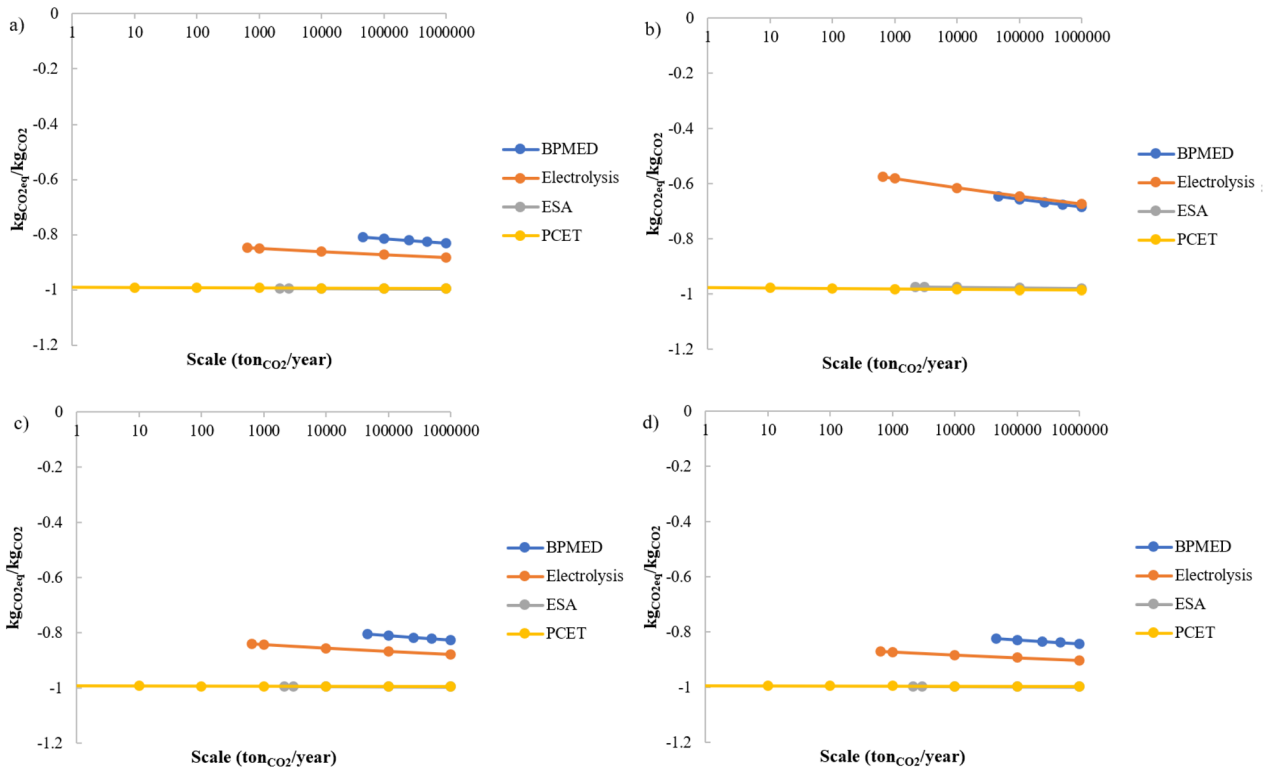

Fig. 14 Environmental burden of e-DAC technologies located in Europe when (a) nuclear, (b) solar, (c) off-shore wind, and (d) on-shore wind energies are used.

Table 4 Results from the TOPSIS analysis simultaneously considering the year, geographic location and energy source

Ranking	e-DAC technology/year/energy source/geographic location	Score
1	PCET, 2050, wind offshore, China	0.997811
2	PCET, 2050, wind onshore, China	0.996499
3	PCET, 2030, wind onshore, China	0.996056
4	PCET, 2023, wind onshore, China	0.995525
5	PCET, 2030, wind offshore, China	0.995147
6	PCET, 2023, wind offshore, China	0.988941
7	PCET, 2050, wind onshore, US	0.987524
8	PCET, 2030, wind onshore, US	0.986835
9	PCET, 2023, wind onshore, US	0.986816
10	PCET, 2050, wind offshore, US	0.9848

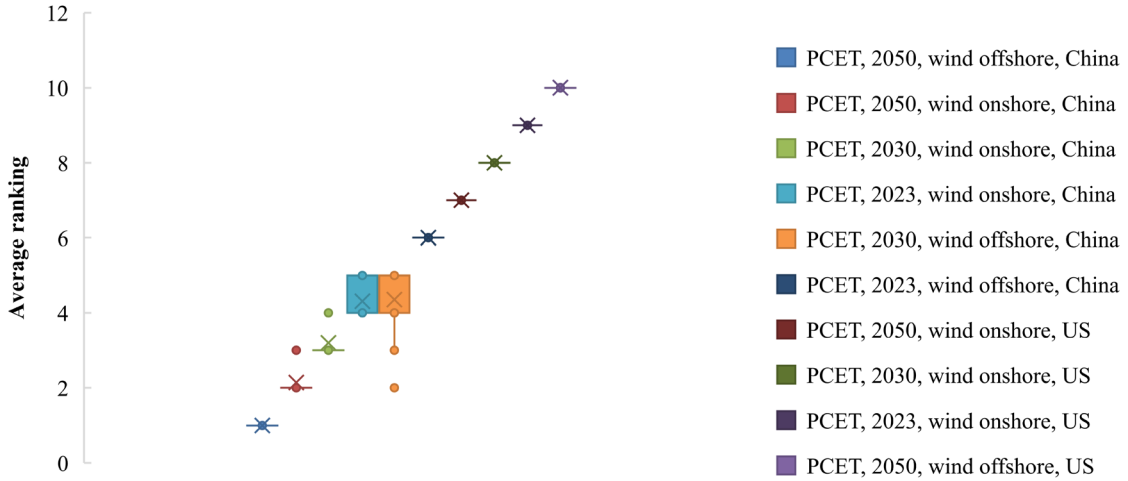

Fig. 15 Average ranking of e-DAC technologies at different years, locations and energy sources in the Monte Carlo simulation of TOPSIS analysis (50% variation of weights).

In this period, a deep construction and spread of this technology is suggested after an initial period of learning. Currently, economic incentives are required to support the construction of electrically driven systems that capture CO_2 from the air. This is in agreement with the unique economic analysis reported in the literature.[41] Economic incentives are needed today to speed up the installation of these processes and hence support learning. Waiting until the years 2040–2050 for their deep construction would be too late and would not enable the zero emissions target by the end of the century. Among renewable energy sources, wind energy is the best resource to produce electrical energy, ensuring the best trade-off among costs, environmental burden, and potential for health and safety. The advantages of wind energy include good conversion efficiency; since wind is consistent in the medium and long-term, the environmental impact is minimal, wind is truly economical, maintenance is simple and only occasionally necessary, and there is excellent circularity in the end-of-life phase.

Table S2 of the SI shows the ranking for all alternatives: the worst case is related to the electrolysis-based process, exploiting nuclear energy built in Europe in 2023.

The stability of the TOPSIS analysis ranking is checked by changing both the electricity price and learning rate in the range between ±20% of the nominal case. Results show that the most sustainable e-DAC system is that based on the PCET, as reported in Tables S3 and S4 of the SI.

A Monte Carlo simulation is conducted by changing weight values between 10% and 50% of the nominal case. Fig. 15 reports the results for a variation of 50%, while Fig. S1–S4 in the SI show results for the other percentages. It is possible to see that the weight variation does not affect the ranking position value. Moreover, that weight variation is not particularly significant for the average ranking position; small variations are obtained compared to the nominal case.

4 Conclusions

Herein, we report a comparison of different fully electrified DAC technologies: electrolysis and BPMED, PCET, and ESA. After modelling the scale-up of these systems through a hybrid learning curve method, total costs and global warming potential in terms of $kg_{CO_2\ eq}\ kg_{CO_2}^{-1}$ captured are evaluated as a function of the plant scale for different times (2023, 2030, 2050), energy

sources (nuclear, off-shore and on-shore wind, solar), and geographical areas (US, China, and Europe). The results show that for all the investigated regions, the BPMED and electrolysis systems are characterized by higher costs and environmental impact, while ESA and PCET processes have lower costs and emissions. For all technologies, in the future, lower total costs are anticipated, partly due to a lower price of renewable electricity. For the US region, in the year 2050, the highest cost is for the electrolysis-based process moved by nuclear energy (1107 $ per ton_{CO_2} for a capture capacity of 1 $Mton_{CO_2}$ per year), while the lowest cost is for PCET driven by electricity generated by onshore wind energy (66 $ per ton_{CO_2} for a capture capacity of 1 $Mton_{CO_2}$ per year). For the European Union region, in the year 2050, the electrolysis-based process will still be the most expensive if driven by nuclear energy (1297 $ per ton_{CO_2} for a capture capacity of 1 $Mton_{CO_2}$ per year), while PCET will be the cheapest if powered by solar energy ($73 per ton_{CO_2} for a capture capacity of 1 $Mton_{CO_2}$ per year). On the other hand, for China in the future (2050), the e-DAC process using an electrolytic cell and exploiting nuclear energy will lead to the highest cost ($711 per ton_{CO_2} for a capture capacity of 1 $Mton_{CO_2}$ per year), and PCET using solar energy will be the most effective ($44 per ton_{CO_2} for a capture capacity of 1 $Mton_{CO_2}$ per year). Regarding the environmental burden, in the US the use of solar energy to produce electricity causes the highest impact for the electrolysis-based process (−0.47 $kg_{CO_2\ eq}\ kg_{CO_2}^{-1}$ captured for a plant scale of 1 $Mton_{CO_2}$ per year), while on-shore wind ensures the lowest impact for PCET (−0.996 $kg_{CO_2\ eq}\ kg_{CO_2}^{-1}$ captured for a plant scale of 1 $Mton_{CO_2}$ per year). For China, the same technologies as for the US have the highest and lowest environmental burdens: electrolysis if powered by solar energy (−0.43 $kg_{CO_2\ eq}\ kg_{CO_2}^{-1}$ captured for a plant scale of 1 $Mton_{CO_2}$ per year), and PCET if powered by nuclear energy (−0.996 $kg_{CO_2\ eq}\ kg_{CO_2}^{-1}$ captured for a plant scale of 1 $Mton_{CO_2}$ per year). The same results are seen for the European Union: the electrolysis-based process driven by solar energy and PCET moved by on-shore wind will lead to −0.67 and −0.996 $kg_{CO_2\ eq}\ kg_{CO_2}^{-1}$ captured, respectively, to capture 1 $Mton_{CO_2}$ per year. The TOPSIS method is applied to determine the best sustainable e-DAC process, and it indicated that PCET is the best solution if located in China in the future (2040–2050) and exploiting on-shore wind energy to generate electricity. This implies that significant economic incentives are currently required for the roll-out of these processes. In the future, a more accurate and complete LCA analysis (from cradle-to-gate system boundaries) of these technologies is suggested to be carried out.

Overall, these results provide some practical guidance for the future development of electrochemical DAC systems. Among all e-DAC technologies, it is suggested that ESA or pH-swing electrolysis can be prioritized for reversibility and energy efficiency, avoiding the use of rare or toxic materials (*e.g.*, silver, cobalt). The use of abundant, non-critical materials is preferred for global scalability.

Since PCET is the most promising solution, it would be better to optimize the redox-active carrier for selectivity, capacity, and reversibility by designing redox-tunable materials with high CO_2 binding capacity at low partial pressure, improving chemical stability across thousands of cycles, and exploring solid-state and hybrid ion-conducting materials that eliminate the need for volatile solvents.

Regarding the environmental analysis, net emissions should be minimized across the supply chain, manufacturing, and disposal, and water and land use should be addressed. Since the e-DAC systems work with integrated renewable energy, it is important to reduce energy consumption and increase process compatibility with renewable power. In this context, it is suggested that power buffering strategies or hybrid energy storage be used, and work should be conducted at low voltage.

As additional guidance for future development, a realistic techno-economic assessment should be performed based on pilot-scale data. Inside the economic analysis, it would be useful to develop proper policy support, providing incentives for durable carbon removal.

Author contributions

Grazia Leonzio: conceptualization, methodology, investigation, data curation, visualization, formal analysis, writing – original draft, writing – review and editing. Nilay Shah: supervision, writing – review and editing.

Conflicts of interest

There are no conflicts to declare.

Data availability

The data supporting the findings of the study are available within the paper and its SI. See DOI: **https://doi.org/10.1039/d5su00227c**.

Acknowledgements

The authors would like to thank the University of Cagliari for funding the work and the Imperial College London for allowing them to develop the work during the visiting research period.

References

1 G. L. Foster and E. J. Rohling, Relationship between sea level and climate forcing by CO 2 on geological timescales, *Proc. Natl. Acad. Sci. U. S. A.*, 2013, **110**(4), 1209–1214.
2 Our world in data, 2024, **https://ourworldindata.org/co2-and-greenhouse-gas-emissions**.
3 Climate.gov, 2024, **https://www.climate.gov/news-features/featured-images/2024-was-warmest-year-modern-record-globe**.
4 Z. Hausfather, Bounding the climate viability of natural gas as a bridge fuel to displace coal, *Energy Policy*, 2015, **86**, 286–294.
5 J. E. Chae, J. Choi, D. Lee, S. Lee and S. Kim, Development of anion exchange membrane-based electrochemical CO_2 separation cells for direct air capture, *J. Ind. Eng. Chem.*, 2024, **145**, 543–550.

6 C2ES, 2024, https://www.c2es.org/content/carbon-dioxide-removal/.
7 A. Galan-Martín, D. Vazquez, S. Cobo, N. Mac Dowell, J. A. Caballero and G. Guillen-Gosalbez, Delaying carbon dioxide removal in the European Union puts climate targets at risk, *Nat. Commun.*, 2021, **12**, 6490.
8 T. Gasser, C. Guivarch, K. Tachiiri, C. D. Jones and P. Ciais, Negative emissions physically needed to keep global warming below 2 °C, *Nat. Commun.*, 2015, **6**, 7958.
9 J. Lezaun, P. Healey, T. Kruger and S. M. Smith, Governing Carbon Dioxide Removal in the UK: Lessons Learned and Challenges Ahead, *Front. Clim.*, 2021, **3**, 673859.
10 J. Strefler, N. Bauer, F. Humpenoder, D. Klein, A. Popp and E. Kriegler, Carbon dioxide removal technologies are not born equal, *Environ. Res. Lett.*, 2021, **16**, 074021.
11 IEAGHG, *Assessing the Techno-Economic Performance, Opportunities and Challenges of Mature and Nearly-Mature Negative Emissions Technologies (NETs)*, 2021.
12 G. Leonzio, P. S. Fennell and N. Shah, Analysis of Technologies for Carbon Dioxide Capture from the Air, *Appl. Sci.*, 2022, **12**, 8321.
13 H. Xu, L. Yu, C. Chong and F. Wang, A comprehensive review on direct air carbon capture (DAC) technology by adsorption: From fundamentals to applications, *Energy Convers. Manage.*, 2024, **322**, 119119.
14 X. Zhu, W. Xie, J. Wu, Y. Miao, C. Xiang, C. Chen, B. Ge, Z. Gan, F. Yang, M. Zhang, D. O'Hare, J. Licef, T. Ge and R. Wang, Recent advances in direct air capture by adsorption, *Chem. Soc. Rev.*, 2022, **51**, 6574–6651.
15 A. Sodiq, Y. Abdullatif, B. Aissa, A. Ostovar, N. Nassar, M. ElNaas and A. Amhamed, A review on progress made in direct air capture of CO2, *Environ. Technol. Innovat.*, 2023, **29**, 102991.
16 B. Gurkan, X. Su, A. Klemm, Y. Kim, S. S. Sharada, A. Rodriguez-Katakura and K. J. Kron, Perspective and challenges in electrochemical approaches for reactive CO2 separations, *iScience*, 2021, **24**, 103422.
17 M. Rahimi, A. Khurram, T. A. Hatton and B. Gallant, Electrochemical carbon capture processes for mitigation of CO2 emissions, *Chem. Soc. Rev.*, 2022, **51**, 8676.
18 R. Sharifian, R. M. Wagterveld, I. A. Digdaya, C. Xiang and D. A. Vermaas, Electrochemical carbon dioxide capture to close the carbon cycle, *Energy Environ. Sci.*, 2021, **14**, 781.
19 H. Bouaboula, J. Chaouki, Y. Belmabkhout and A. Zaabout, Comparative review of Direct air capture technologies: From technical, commercial, economic, and environmental aspects, *Chem. Eng. J.*, 2024, **484**, 149411.
20 F. Sabatino, M. Gazzani, F. Gallucci and M. v. S. Annaland, Modeling, Optimization, and Techno-Economic Analysis of Bipolar Membrane Electrodialysis for Direct Air Capture Processes, *Ind. Eng. Chem. Res.*, 2022, **61**, 12668–12679.
21 Mission Zero Tech, 2024, https://www.missionzero.tech/lab-notes/electrochemical-direct-air-capture#:~:text=Thisheat%2Dfreeandfully,releasetriggerssuchashumidity.
22 S. Kim, H. Shin and J. S. Kang, Electrochemical reduction of captured CO2: A route toward the integrated carbon capture and utilization, *Curr. Opin. Electrochem.*, 2023, **40**, 101321.
23 Verdox, 2024, https://verdox.com/.
24 RedoxNRG, 2024, https://www.redoxnrg.com/.
25 Repair, 2024, https://www.repair-carbon.com/technology.
26 Carbon Atlantis, 2024, https://phlair.com/carbon-atlantis-is-now-phlair.
27 E-quester, 2024, https://e-quester.com/.
28 A. Hemmatifar, J. S. Kang, N. Ozbek, K. J. Tan and T. A. Hatton, Electrochemically Mediated Direct CO2 Capture by a Stackable Bipolar Cell, *ChemSusChem*, 2022, **15**, e202102533.
29 S. Voskian and T. A. Hatton, Faradaic electro-swing reactive adsorption for CO2 capture, *Energy Environ. Sci.*, 2019, **12**, 3530.
30 H. Xie, Y. Wu, T. Liu, F. Wang, B. Chen and B. Liang, Low-energy-consumption electrochemical CO2 capture driven by biomimetic phenazine derivatives redox medium, *Appl. Energy*, 2020, **259**, 114119.
31 S. Jin, M. Wu, Y. Jing, R. G. Gordon and M. J. Aziz, Low energy carbon capture via electrochemically induced pH swing with electrochemical rebalancing, *Nat. Commun.*, 2022, **13**, 2140.
32 X. Jin, S. Jin, L. Li, R. Gordon, P. Wang, M. J. Aziz and Y. Ji, Direct air capture of CO2 in a hybrid electrochemical flow cell, 2024, https://chemrxiv.org/engage/api-gateway/chemrxiv/assets/orp/resource/item/666c602601103d79c53758cc/original/direct-air-capture-of-co2-in-a-hybrid-electrochemical-flow-cell.pdf.
33 S. Jin, M. Wu, R. G. Gordon, M. J. Aziz and D. G. Kwabi, pH swing cycle for CO2 capture electrochemically driven through proton-coupled electron transfer, *Energy Environ. Sci.*, 2020, **13**, 3706.
34 H. Seo, M. P. Nitzsche and T. A. Hatton, Redox-Mediated pH Swing Systems for Electrochemical Carbon Capture, *Acc. Chem. Res.*, 2023, **56**, 3153–3164.
35 H. Seo and T. A. Hatton, Electrochemical direct air capture of CO2 using neutral red as reversible redox-active material, *Nat. Commun.*, 2023, **1**(4), 313.
36 Q. Shu, L. Legrand, P. Kuntke, M. Tedesco and H. V. M. Hamelers, Electrochemical Regeneration of Spent Alkaline Absorbent from Direct Air Capture, *Environ. Sci. Technol.*, 2020, **54**, 8990–8998.
37 A. P. Muroyama and L. Gubler, Carbonate Regeneration Using a Membrane Electrochemical Cell for Efficient CO2 Capture, *ACS Sustainable Chem. Eng.*, 2022, **10**, 16113–16117.
38 Q. Shu, C. S. Sin, M. Tedesco, H. V. M. Hamelers and P. Kuntke, Optimization of an electrochemical direct air capture process with decreased CO2 desorption pressure and addition of background electrolyte, *Chem. Eng. J.*, 2023, **470**, 144251.
39 H. M. Almajed, R. Kas, P. Brimley, A. M. Crow, A. Somoza-Tornos, B. M. Hodge, T. E. Burdyny and W. A. Smith, Closing the Loop: Unexamined Performance Trade-Offs of Integrating Direct Air Capture with (Bi)carbonate Electrolysis, *ACS Energy Lett.*, 2024, **9**, 2472–2483.

40 G. Liu, A. Yang and R. C. Darton, Numerical Modeling and Comparative Analysis of Electrolysis and Electrodialysis Systems for Direct Air Capture, *ACS Sustainable Chem. Eng.*, 2024, **12**, 3951–3965.
41 J. Young, N. McQueen, C. Charalambous, S. Foteinis, O. Hawrot, M. Ojeda, H. Pilorge, J. Andresen, P. Psarras, P. Renforth, S. Garcia and M. v. d. Spek, The cost of direct air capture and storage can be reduced via strategic deployment but is unlikely to fall below stated cost targets, *One Earth*, 2023, **6**, 899–917.
42 F. Sabatino, M. Mehta, A. Grimm, M. Gazzani, F. Gallucci, G. J. Kramer and M. v. s. Annaland, Evaluation of a Direct Air Capture Process Combining Wet Scrubbing and Bipolar Membrane Electrodialysis, *Ind. Eng. Chem. Res.*, 2020, **59**, 7007–7020.
43 H. M. Almajed, R. Kas, P. Brimley, A. M. Crow, A. Somoza-Tornos, B. M. Hodge, T. E. Burdyny and W. A. Smith, Closing the Loop: Unexamined Performance Trade-Offs of Integrating Direct Air Capture with (Bi)carbonate Electrolysis, *ACS Energy Lett.*, 2024, **9**, 2472–2483.
44 S. Roussanaly, N. Berghout, T. Fout, M. Garcia, S. Gardarsdottir, S. M. Nazir, A. Ramirez and E. S. Rubin, Towards improved cost evaluation of Carbon Capture and Storage from industry, *Int. J. Greenh. Gas Control*, 2021, **106**, 103263.
45 ThuinderSaidEnergy, 2024, **https://thundersaidenergy.com/downloads/fans-and-blowers-costs-and-energy-consumption/**.
46 K. Mongird, V. Viswanathan, J. Alam, C. Vartanian and V. Sprenkle, Grid Energy Storage Technology Cost and Performance Assessment, Technical Report Publication No. DOE/PA-0204 December 2020, 2020, **https://www.energy.gov/energy-storage-grand-challenge/articles/2020-grid-energy-storage-technology-cost-and-performance**.
47 IEA, World Energy Outlook 2023, 2023, **https://www.iea.org/reports/world-energy-outlook-2023**.
48 Y. Hu, R. Gani, K. Sundmacher and T. Zhou, Assessing the future impact of 12 direct air capture technologies, *Chem. Eng. Sci.*, 2024, **298**, 120423.
49 Ecoinvent, 2020, **https://ecoinvent.org/**.
50 DSM, 2024, **https://www.dsm.com/content/dam/protected/personal-care/en_US/vitamins/vitamins_distributor/niacinamide-pc_presentation_2021-01.pdf**.
51 M. Madanchian and H. Taherdoost, A comprehensive guide to the TOPSIS method for multi-criteria decision making, *Sustain. Soc. Dev.*, 2023, **1**, 1–6.
52 A. Heidari, H. Boleydei, A. Rohani, H. R. Lu and H. Younesi, Integrating life cycle assessment and life cycle costing using TOPSIS to select sustainable biomass-based -carbonaceous adsorbents for CO2 capture, *J. Clean. Prod.*, 2022, **357**, 131968.
53 K. L. Wen, T. C. Chang and M. L. You, The grey entropy and its application in weighting analysis, *IEEE Int. Conf. Syst. Man Cybern.*, 1998, **2**, 1842–1844.
54 J. J. Shuai and W. W. Wu, Evaluating the influence of E-marketing on hotel performance by DEA and grey entropy, *Expert Syst. Appl.*, 2011, **38**, 8763–8769.
55 F. Parvaneh and A. Hammad, Application of Multi-Criteria Decision-Making (MCDM) to Select the Most Sustainable Power-Generating Technology, *Sustainability*, 2024, **16**, 3287.
56 Our world in data, 2024, **https://ourworldindata.org/safest-sources-of-energy#:~:text=Thekeyinsightisthat,solararejustassafe**.
57 K. A. Pacheco, A. E. Bresciani and R. M. V. Alves, Multi criteria decision analysis for screening carbon dioxide conversion products, *J. CO_2 Util.*, 2021, **43**, 101391.
58 N. Rosen, A. Welter, M. Schwankl, N. Plumere, J. Staudt and J. Burger, Assessment of the Potential of Electrochemical Steps in Direct Air Capture through Techno-Economic Analysis, *Energy Fuels*, 2024, **38**, 15469–15481.
59 MIT, 2024, **https://news.mit.edu/2020/new-approach-to-carbon-capture-0709**.